Water Resources and Industry 30 (2023) 100220

Contents lists available at ScienceDirect

Water Resources and Industry

journal homepage: www.elsevier.com/locate/wri

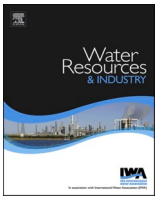

Degradation of Rhodamine dyes by Advanced Oxidation Processes (AOPs) – Focus on cavitation and photocatalysis - A critical review

Ashish V. Mohod [a,b], Malwina Momotko [c], Noor Samad Shah [d], Mateusz Marchel [e], Mohammad Imran [f], Lingshuai Kong [g], Grzegorz Boczkaj [e,h,*]

[a] Department of Chemical Engineering, AISSMS College of Engineering, Kennedy Road, Pune, 411001, India
[b] Chemical Engineering Departament, Universidade de São Paulo, São Paulo, Brazil
[c] Department of Process Engineering and Chemical Technology, Faculty of Chemistry, Gdansk University of Technology, Gdansk, St.11/12, 80-233, Poland
[d] Department of Environmental Sciences, COMSATS University Islamabad, Vehari Campus, 61100, Pakistan
[e] Department of Sanitary Engineering, Faculty of Civil and Environmental Engineering, Gdansk University of Technology, Gdansk, St.11/12, 80-233, Poland
[f] Centre for Inorganic Chemistry, School of Chemistry, University of the Punjab Lahore, 54000, Pakistan
[g] Institute of Eco-Environmental Forensics, School of Environmental Science and Engineering, Shandong University, Qingdao, 266237, China
[h] Eko Tech Center, Gdansk University of Technology, Gdansk, St.11/12, 80-233, Poland

ARTICLE INFO

Keywords:
Emerging organic pollutants
Radical reactions
Catalytic oxidation
Textile industrial effluents
Ultraviolet
Ecotoxicity

ABSTRACT

This review evaluates selected advanced oxidation processes (AOPs) - cavitation and photocatalysis - successfully used for wastewater treatment towards degradation of Rhodamine (Rh) dyes. Reactor configuration and impact of process parameters and oxidants addition (hydrogen peroxide, ozone, persulfates) on degradation effectiveness along with degradation mechanisms are discussed. Best technologies provide 100% degradation within 10–30 min. Rhodamine B is effectively degraded in highly acidic conditions (pH 2), while Rhodamine 6G requires basic conditions (pH 10). The most effective oxidants were hydrogen peroxide and ozone. Ecological Structure Activity Relationships (ECOSAR) revealed acute toxicities of the intermediates and by-products of the Rh dye.

1. Introduction

The disposal of coloured wastewater is a significant challenge for the industry but also a risk to the surrounding ecosystem. The presence of dyes in wastewater can be a significant contributor to environmental pollution. The pollution of freshwater resources is one of the largest environmental effects of colors in the fashion industry. The garment business uses almost 93 billion cubic meters of water annually, which is enough to fill 37 million Olympic swimming pools, according to the Ellen MacArthur Foundation [1]. The use of dyes is the single largest contributor to the waste of water. As a result, dyeing processes are among the most energy and pollution-intensive aspects of our clothing. A pair of jeans is a good illustration of this issue. A single pair of jeans requires, from the growth of the raw cotton to the finished product, roughly 7,500 L of water [2,3]. The yarn or fabric is repeatedly dipped into large vats of synthetic indigo dye to give the jeans their blue colour. During traditional methods of processing textiles, up to 2,000 different

* Corresponding author. Gdansk University of Technology, Faculty of Civil and Environmental Engineering, Department of Sanitary Engineering, 80 – 233, Gdansk, G. Narutowicza St. 11/12, Poland.
E-mail address: grzegorz.boczkaj@pg.edu.pl (G. Boczkaj).

https://doi.org/10.1016/j.wri.2023.100220
Received 2 February 2023; Received in revised form 2 June 2023; Accepted 14 July 2023
Available online 21 July 2023

chemicals are used. Toxic substances like mercury, formaldehyde, or chlorine are used in this process [4]. The accumulation of dyes in the water to the extent that light cannot reach the surface hinders the ability of plants to photosynthesize. This reduces the oxygen content of the water, causing aquatic life and plants to perish [5].

The Rhodamine compounds are important family of dyes, its types are given Fig. 1. Because of Rh dyes greater chemical stability, Rh B and Rh 6G are the members of the Rhodamine family that are utilized the most frequently in a variety of applications. According to the Industry ARC (industry research council) report, the worldwide production of Rhodamine dyes is estimated to reach $232.5 million by 2027 during the forecast period 2022–2027. The physical and chemical properties of Rh B and Rh 6G have been given in Supplementary Table ST1.

Rhodamine B (Rh B), also called Basic Violet 10, is a bright reddish violet color that is non-volatile and dissolves easily in water. It is one of the most significant xanthene dyes and is utilized in the dying of cotton, bamboo, weed, and leather, as well as the preparation of ball pen and stamp pad inks [6,7]. Rhodamine 6G (Rh 6G) is an organic, basic dye that is dark reddish purple in color. It is widely used as a tracer to find out the characteristics of flow properties, fluorescence, and diagnostic tools in medicine and plant pathology, and is also used to color wool, cotton, silk, and papers [8,9]. Both dyes are highly water-soluble and are used in biological stains, fireworks, and color tracers in herbicides, which results in the chemical's release into the surrounding environment. Even Rh B is used as an illegal food ingredient which is added in chilli sauce and candies in a number of underdeveloped countries [10]. Both Rh dyes can induce respiratory injury, tissue necrosis, reproductive system harm, and even cancer in aquatic creatures [11]. The discharge of Rh dye effluents into natural ecosystems is not only harmful to aquatic life, but it can also, in many instances, cause genetic mutations in humans [12,13]. When ingested, it is toxic, and it also irritates the skin, the eyes, and the respiratory tract [14,15]. As a result, it is crucial to treat effluents that contain these chemicals in order to protect the ecosystem and water in general. Rh B is difficult to biodegrade, which is one of the reasons it contributes to the ongoing pollution of the environment. In light of these concerns and reported trends, the number of articles on the degradation of Rh dyes in Scopus also increases every year (Supplementary Figure, SF1), which reflects that the environmental impact of Rh dyes is receiving high attention in the community.

According to Kuo and Ho (2001) [16] and Sun et al. (2007) [17], biological degradation is generally ineffective for dye pollution. Studies based on conventional methods such as activated sludge [18], coagulation, activated charcoal [19], adsorption [15,20], membrane filtration, etc. [21], can generally be utilized efficiently to remove colors from the effluents of industries [22–24]. In spite of this, these methods are regarded as non-destructive because they only transfer color from liquid to solid waste except in the case of membrane techniques, the retentate by-product is in liquid form [25]. Numerous researchers have developed and reported advanced oxidation processes (AOPs) for the purpose of degrading organic compounds in wastewater. Some examples of these processes are ozonation [26], Fenton reagent [27], hydrogen peroxide [28], photo-Fenton [27], photo-ozone [29], photo-hydrogen peroxide [30], and photo-catalysts [31–36]. The focus of the present work is on the applications of alternative/emerging AOPs for the effective treatment of wastewaters that contain Rh dyes, especially Rh B and Rh 6G. These treatment schemes are based on the employment of ultrasonic, UV irradiation, and hydrodynamic cavitation as the primary treatment agents. A critical review based on such a wastewater treatment scheme, which contains two commercially important Rh dyes (Rh B and Rh 6G), to our knowledge, never has been discussed before in this work. This study is one of the few that elaborates the degradation of the most important industrial hazardous chemical compounds in wastewater using a combination of AOPs and external oxidants. Herein, the focus is provided on photocatalysis and

Fig. 1. Prominent chemical compounds associated with Rhodamine dye family.

cavitation based processes that in many cases gave very effective treatment.

It is intended to describe the results in an effective manner in order to establish the general principles for treating wastewater containing Rh dyes using advanced oxidation processes, which have lately gained greater attention from the researchers and have several benefits. Because of this, the primary emphasis of this review is on performing an in-depth analysis of all of the operating parameters that can have an impact on ultrasonic irradiation, ultraviolet irradiation, and hydrodynamic cavitation, with the following goals in mind: i) to study the effect of various operating parameters based on ultrasonic and ultraviolet irradiation along with hydrodynamic cavitation in an efficient way; ii) to define the general outline for the operating reaction parameters based on advanced oxidation processes via cavitational and ultraviolet irradiation techniques in order to achieve the desired level of intensification; iii) to intensify the process of treatment more efficiently with the help of catalysts and additives. iv) to design reactors for large amounts of Rh dye-containing wastewater in a cost-effective approach. This study gives a brief review that investigates the decomposition of the most significant industrially hazardous chemical compounds, particularly Rh dyes family, that may be found in wastewater by utilizing a mix of AOPs and external oxidants, in addition to the numerous different cavitational reactors that might be utilized.

2. Types of treatment

2.1. Ultrasonic cavitation

In order to produce ultrasonic cavitation, high-frequency (20 kHz–1 MHz) sound waves must be passed through the liquids [37]. When ultrasound flows through a liquid medium, it causes the continuum to go through a rarefaction and compression cycle. When these cycles alternate, cavitation and radical production occur as a result of the release of local energy, which triggers the following chain of reactions [38]:

$$H_2O + \overset{)))US}{\longrightarrow} H^+ + OH^* \quad (1)$$

$$O_2 +))) \overset{)))US}{\longrightarrow} 2O^- \quad (2)$$

$$O^- + H_2O \overset{)))US}{\longrightarrow} 2OH^* \quad (3)$$

$$H^+ + O_2 \overset{)))US}{\longrightarrow} OH^* + O \quad (4)$$

$$H^+ + O_2 \overset{)))US}{\longrightarrow} HO_2^- \quad (5)$$

The various radicals include hydroxyl radicals (OH^*), hydrogen atoms (H^+), oxygen atoms (O^-), and hydroperoxyl radicals (HO_2^*), and the ')))' indicates ultrasonic waves. The two most common processes for the decomposition of any contaminants in the wastewater are free radical reactions and pyrolysis. Many examples of chemical contaminants removed from wastewater using ultrasound cavitation have been reported in the literature [36,39–43].

The ultrasonic probe or horn has been shown to be the most widely used ultrasonic reactor in small volumes of 50 mL–500 mL, where the removal of chemical contaminants is done with greater efficiency [44,45]. Ultrasonic baths have been used in several investigations at higher scales of operation, but the removal of chemical contaminants is less effective [46] as compared to ultrasonic horns. Typically, equipment with a bigger dissipation area provides greater energy efficiency at similar levels of input energy (a greater proportion of the total supplied electrical energy is transformed into positive effects) [47]. Furthermore, the use of equipment based on multiple frequencies/multiple transducers (devices used for converting supplied electrical energy into sound energy and producing ultrasound with frequencies ranging from 15 kHz to 10 MHz) has been shown to be more beneficial than equipment based on a single frequency [37,48]. Another new development with a promising future for medium-to large-scale applications are ultrasonic horns vibrating in radial directions [49], which also have the advantage of better energy dissipation due to a larger irradiating area, but more work is required in terms of testing this equipment for operation at high frequency and high-power dissipation [50]. To enhance the removal efficiency of chemical contaminants from wastewater, all of these operating factors need to be optimized: the pH at which contaminants are introduced, the concentration of contaminants, operating temperature, ultrasonic frequency, and power density.

2.2. Hydrodynamic cavitation

Another type of cavity formation that occurs when local fluid pressure decreases as fluid velocity increases due to a flow restriction is known as hydrodynamic cavitation. When this pressure drops below its critical value, which is usually the vapor pressure of the liquid medium at a certain operating temperature, small cavities filled with vapor form in the fluid. At this point, the cavitation bubbles may be seen and are called cavitation inception [51]. With an increase in fluid velocity, pressure drops even further, increasing the cavitation intensity. The cavitational consequences of hydrodynamic cavitation are influenced by the creation of many cavities and the impact of turbulence [52,53].

Orifice, venturi (slit or circular), high-speed homogenizer, whirling jet, vortex diodes etc. can all be used as cavitating devices in hydrodynamic cavitation set up to generate cavitation [54–58]. Fig. 2 depicts a different hydrodynamic cavitational reactor used in various applications till the date. Hydrodynamic cavitation has a number of advantages over acoustic cavitation, including increased

cavitational yield, improved energy economy, simplicity of operation, and the capacity to treat a larger volume of solution [59,60].

2.3. Photocatalysis

As a consequence of their ability to completely mineralize organic pollutants while operating under moderate temperature and pressure conditions, photocatalytic or photochemical degradation technologies are becoming more and more important in the

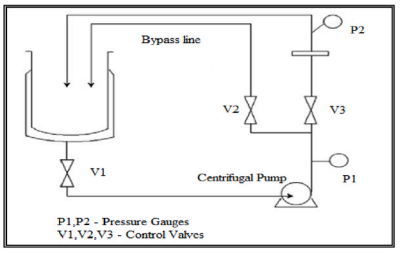

Hydrodynamic cavitation

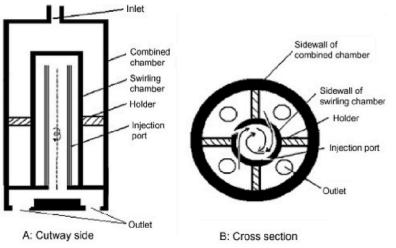

Swirling cavitation reactor

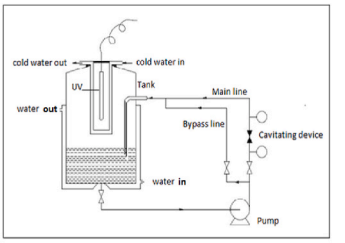

Combined UV and Hydrodynamic cavitation reactor

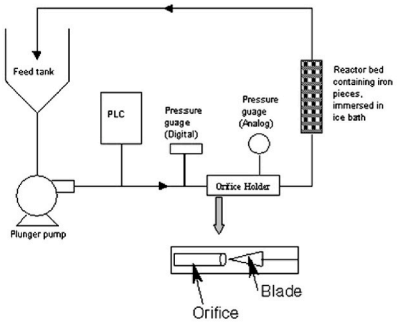

Liquid whistle reactor

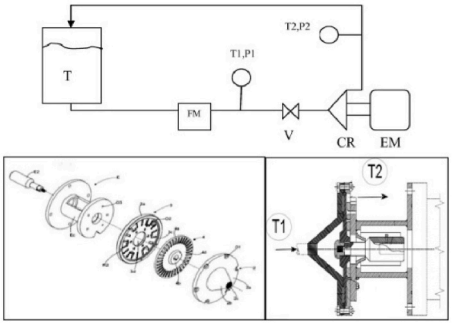

High-speed homogenizer

T = tank, FM = flowmeter, V = valve, CR = cavitation reactor, EM = electric motor, Ti,Pi = temperature and pressure measurements.

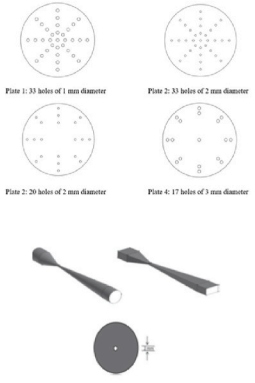

Multiple-orifice plates and venturi

Fig. 2. Depicts a different hydrodynamic cavitational reactor used in various applications.

wastewater treatment industry due to their low cost and environmental sustainability [61,62], especially when solar irradiation is used. When a photon of the right energy level interacts with the molecules of the chemical species present in a solution, either with or without a catalyst, a free radical process is initiated. Free radical process involves creation of highly reactive species like hydroxyl radicals. The photocatalytic process found at the surface of semiconductors, such as titanium dioxide, is an alternate method of obtaining free radicals and does, in fact, significantly speed up their production and, thus, the rate of oxidative degradation [63,64]. As electrons and holes are created whenever a semiconductor catalyst is exposed to UV light, as demonstrated in the reaction mechanism [65], electron excitation from the valence band (VB) to the conduction band (CB) occurs.

$$TiO_2 + hv \rightarrow e_{CB-} + h_{VB+} \quad (6)$$

$$h_{VB} + OH^- \rightarrow OH^* \quad (7)$$

$$h^+_{VB} + H_2O(ads) \rightarrow OH^* + H^+ \quad (8)$$

$$e_{CB-} + O_2 \rightarrow O_2^{-*} \quad (9)$$

A photocatalyst's positive holes oxidize water to create hydroxyl radicals (OH^*) that have a high oxidative capacity, which can then react with organic compounds [66].

To perform the photocatalytic process, tiny particles of solid semiconductor distributed in the liquid phase of a reactor that is irradiated with UV light may be used. This may be done using either mechanical or magnetic stirrers, depending on your needs. To meet the first requirement, commercial photocatalytic items can be deposited onto the surface, although they can be easily eroded by the running liquid. The crystalline structure of the end product and hence the catalytic activity may be difficult to regulate when using physical or chemical vapor deposition methods to produce supported films. There are several benefits of using immobilized or supported catalytic reactors. The main aspect relates to the fact that the supported catalyst does not have to be separated from the fluid, which eliminates the need for ultrafine particle filtration. A variety of configurations may be used, but the most essential thing is to

Table 1
Degradation process optimization parameters based on reactor configuration.

Name of reactor/ Rhodamine	Parameter	Specification	Operating parameter	Results	Reference
HC (Multiple orifice)/Rh B	Inlet pressure	Centrifugal pump (2900 rpm, 5.5 kW, Diameter of orifice 1 mm, number of holes 32, thickness of plate 1 mm.	2.4–5.8 bar (5 mg/L of the initial dye concentration using a couple of orifice plates type (A))	Decolorization of 61% at 5.8 bars (Cv 0.27)	[67]
HC (Circular Venturi and orifice)/Rh B		4 L, reciprocating pump, 1.1 kW	2.9–5.8 bar (Circular venturi (2 mm), orifice (2 mm diameter, pH 4.78, 10 ppm)	Degradation at 4.8 bar 25% using venturi (Cv 0.1) and 22% using orifice (Cv 0.1)) in 120 min	[68]
HC (circular/slit venturi)/Rh 6G		6L, Piston pump (2.2 kW), Circular (2 mm) and slit (W 3.14 mm, H 1 mm, B 1 mm)	3–11 bar (10 ppm, pH 10.0)	Degradation of 32.06% and 29.65% at 5 bars for slit (Cv 0.07) and circular venturi (Cv 0.11), resp. in 120 min	[69]
HC (circular Venturi)/Rh B		4 L, centrifugal pump (3.0 kW), venturi 2 mm diameter	1–5 bar (pH 3, 10 ppm dye concen, 25°C)	18.5% degradation at pressure of 4 bar after 120 min	[70]
HC/Multi-orifice plate/Rh B		300L, Centrifugal pump (3 kW), 18 orifice holes (2 mm diameter)	1.5–3.0 bar (0.3 g/L of CCl4, pH 3.0, temp 13°C, 10 ppm)	76.84% degradation at 3 bar after 210 min	[71]
HC (Circular and square Venturi)/Rh B	Cavitation number	Circular venturi throat radii RS-1 (0.5 mm), RS-2 (1.0 mm), RS-3 (2 mm), Square venturi (α-2),Square venturi (α-1),Square venturi (α-3)	150 min	58.32% for Square venturi (α-2, 0.10 Cv),	[51]
HC (Multiple orifice)/Rh B		50 l, Centrifugal pump (2900 rpm, 5.5 kW, Orifice plate Plate 2 (8 holes, 2 mm dia.)	30 psig	Effective Plate 2 (Cv 0.2759) after 60 min	[72]
Ultrasonic/Rh B	Ultrasonic power	250 mL, 20 kHz, 3 cm depth of horn	600–1000 W (10 ppm dye concen.)	36.6% degradation at 800 W after 90 min	[70]
Ultrasonic/Rh B		250 mL, 35 kHz 300W,	150, 200, 250 and 300W (20 ppm, Temp 24°C)	Maximum degradation of 98% for 300W after 40 min.	[73]
Ultrasonic/Rh B	Power density	0.5 L, 35 kHz	0.049–0.163 W/mL (5 ppm, Temp 25°C)	Maximum degradation at 0.16 W/mL	[74]
Ultrasonic/Rh B	Frequency	250 mL, 40 kHz 300W,	25, 40, 60 and 80 kHz (20 ppm, Temp 24°C)	Maximum degradation of 98.88% at 40 kHz, after 40 min.	[73]
Ultraviolet/Rh B	UV light power	250 mL, 11, 15 and 26W UV lamps	11, 15 and 26W 5 ppm, 2 pH, 15 min, 0.4 mL H2O2	Maximum degradation of 99.1% at 26W in 15 min	[7]

ensure that the whole active surface gets effectively irradiated.

3. Optimization of process parameters

Following a thorough and comprehensive review of the current literature on hydrodynamic and ultrasonic cavitation as well as photocatalytic oxidation of Rh dyes, the most essential operational parameters that determine the overall degradation efficiency are summarized in Table 1. Below, each aspect of optimization has been discussed.

3.1. Effect of inlet pressure (hydrodynamic cavitation)

Cavitation created by hydrodynamic cavitation is strongly dependent on the reactor's inlet pressure. As a result, numerous researchers have focused on the influence of inlet pressure on the treatment of wastewater or any other application [75–78]. Hydrodynamic cavitation with various cavitating devices has been shown to have an impact on Rh dye degradation by inlet pressure, as shown in the studies described in Table 1. Accordingly, a low inlet pressure values (typically 1–3 bar) are insufficient to enhance degradation [79]; nevertheless, a higher inlet pressure (generally 3–5 bar) can increase degradation; this depends on the type of cavitating device and its geometry [48]. According to the inlet pressure parameter analysis, there is no evidence in the literature that discussed Rh dyes have been completely degraded without addition of catalysts or additives. Parsa and Zonouzian (2013) [67] used a multiple-hole orifice plate for hydrodynamic cavitation to investigate the effect of inlet pressure on the degradation of Rh B (Centrifugal pump, 5.5 kW). The orifice plate with 32 holes of 1 mm diameter was used and reported with an increase in pressure from 2.4 to 5.8 bars, the percent degradation increased from 48% to 61%. In another investigation by Yi et al. (2018) [80] used a venturi tube in the form of a ring that was arranged in three layers, with each layer consisting of six venturi tubes fixed in such a way that it rotates to 30° to convert the jet flow into swirling flow and avoid cavitation erosion on the reactor wall. During the investigation of the degradation of Rh B by hydrodynamic cavitation, it was observed that the degradation rate increased with increasing inlet pressure up to 4 bar and subsequently decreased with further increases to 6 bar. Similar kinds of results were also reported by Rajoriya et al. (2017) [69] during the investigation of degradation of Rh 6G using two different venturis, namely circular (diameter 2 mm) and slit (W = 3.14 mm, H = 1 mm, B = 1 mm) in hydrodynamic cavitation (2.2 kW piston pump). It was also reported that a maximum of 32% decolorization (rate constant of 3.0×10^{-3} min^{-1}) was obtained using a slit venturi (0.07 cavitation number), while 29% decolorization (rate constant of 2.5×10^{-3} min^{-1}) was obtained using a circular venturi (0.11 cavitation number) in 120 min at an optimum inlet pressure of 5 bar.

According to the literature, single-hole orifice plates are commonly used in hydrodynamic cavitation due to their simple design,

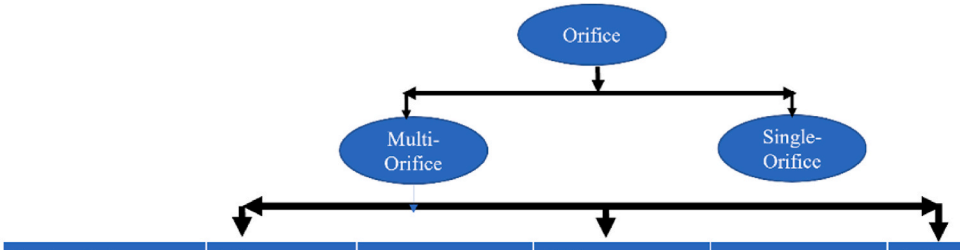

Number of holes	1-10		10-20		20-30	
Diameter of holes	Dia ≤3 mm	Dia ≥4 mm	Dia ≤2 mm	Dia ≥3 mm	Dia ≤1 mm	Dia ≥2 mm
Flow area (mm^2)	Low	High	Low	High	Low	High
α (mm^{-1})	High	Low	High	Low	High	Low
B_0	Low	High	Low	High	Low	High
Total perimeter of holes (mm)	Low	High	Low	High	Low	High
Orifice velocity (m/s)	High	Low	High	Low	High	Low
Cavitation number (Cv)	Low	High	Low	High	Low	High
Degradation (%)	High	Low	High	Low	High	Low

Fig. 3. Hierarchy relationship to understand the degradation rate using orifice plate.

ease of production, and lower cost compared to venturi tubes [81,82]. For maximal pollutant degradation, a larger single-hole orifice plate (no more than 2 mm) is recommended [37]. However, the values of α (throat perimeter/cross-sectional area) and β (throat area/pipe cross-sectional area) are also important. The greater the value of α, the greater the intensity of turbulence and shear layer area, whereas raising the value of β, flow area leads to a rise in cavitational events, leading to higher pollutant degradation [83]. This decrease in cavitation number is due to a decrease in throat cross-section area, which also causes an increase in the fluid velocity in the throat [84]. Studies have shown that employing hydrodynamic cavitation with a single-hole orifice plate can increase pollutant degradation by 30–50%. The reason behind this can be easily understood based on the hierarchical relationship of the orifice plate as described in Fig. 3.

As stated, the maximum cavitational activity in the reactor is determined by the optimum cavitation number; thus, many researchers investigated the effect of inlet pressure as a prerequisite study by modifying the orifice plate into a multiple-hole orifice plate to achieve higher degradation than with a single-hole orifice plate (circular as well as rectangular). According to Fig. 3, the use of multiple-hole orifice plates can lead to higher degradation than single-hole orifice plates. To prevent release of hazardous chemicals into environment, most researchers are exploring strategies to increase degradation using hydrodynamic cavitation without the addition of any other chemicals [31,66,85]. The collapse pressure is affected by the (slit and circular) venturi's flow area, diameter, and rectangular duct. More cavitational effects were observed in rectangular and elliptical venturi [51] compared to circular venturi because of their larger accessible perimeters.

The higher degradation of Rh dye while increasing inlet pressure in cavitating devices, increases the rate of local energy dissipation and the intensity of turbulence [86,87]. As a result, the collapse of cavities rises, resulting in the development of cavitational intensity. This cavitational intensity leads to accelerated dissociation of water molecules into higher amounts of hydroxyl radicals, which results in higher degradation rates until an optimum limit is reached [88]. However, as cavitation number exceeds the optimal value (reaches 0), a large number of cavities arise, filling the whole downstream region of the cavitating device and consolidating to form a bigger cavity [89]. As a result of the random bubble formation, cavities or vapor clouds emerge, causing splashing and vaporization of the flow. This cavity or vapor cloud development is known as choked cavitation or super cavitation [46,90,91], and it results in cushioned cavities with minimal collapse. As a result of the cavities' minimal collapse, cavitational intensity is decreased, and thus smaller amounts of hydroxyl radicals are generated, resulting in lower degradation rates at higher inlet pressures or beyond the optimal limit [81,60,92,93]. Efficient reactor design permits enough free radicals/oxidizing species to be generated at lower operating pressures, reducing energy consumption and operational expenses.

3.2. Effect of cavitation number (hydrodynamic cavitation)

The number of generated cavities and their cavitational intensity largely depend on the inlet pressure and cavitation number. Hence, it is important to study the hydraulic properties of all the cavitating devices, such as orifices and venturis. The cavitation number (C_v) is generally used to characterize the cavitational intensity and degree of cavitation [94,95], and is calculated by Equation (1)

$$C_v = \frac{p_2 - p_v}{(1/2)\rho v^2} \tag{1a}$$

Where P_2 is the fully recovered downstream pressure, P_v is the vapor pressure of the liquid, ρ is the density of the liquid, and v is the velocity at the constriction which can be found out by the main flow rate and orifice diameter. Shivkumar and Pandit (2002) [72], who pointed out that the lower the cavitation number, the higher was the extent of degradation of Rh B using an orifice plate. The multiple hole orifice plate 1 (33 holes, 1 mm diameter) showed a higher cavitation yield of 3.12×10^{-8} (gm of Rh B degraded/joule of energy supplied) for a cavitation number of 0.29. The higher cavitational yield obtained was explained by the author results from a reduction in hole size that reduces the scale of turbulence and raises the turbulent pressure fluctuation frequency, resulting in a more violent collapse of the cavities, which intensifies the cavitational effect and enhances cavitational yield. Furthermore, it was reported that plate 1 generates higher cavitational yields that are two times larger than those of any other plates the author has used. Rajoriya et al. (2017) [69] also reported similar results while studying the effect of the cavitation number on the degradation of Rh 6G using slit and circular venturi. A maximum 32% decolorization (rate constant of 3.0×10^{-3} min^{-1}) was obtained using a slit venturi (0.07 cavitation number), while a 29% decolorization (rate constant of 2.5×10^{-3} min^{-1}) was obtained using a circular venturi (0.11 cavitation number) in 120 min at an optimum inlet pressure of 5 bar. The flow rate of fluid through the main pipeline increases with an increase in the inlet pressure of the venturi and orifices. Consequently, the fluid velocity at the orifice or venturi opening also increases, resulting in a decrease in cavitation numbers (equation (1)) and an increase in the production of cavities, the collapse of which results in a higher extent of degradation.

According to reviewer literature, the optimal cavitation number for degradation is in the range of 0.05–0.4. These values are typical compared to other organic species degraded under cavitation conditions. Additionally, it should be mentioned that venturis yield better degradation effects than orifice plates due to their ability to achieve lower cavitation numbers. Also, a too low cavitation number (close to 0, typically below 0.05) results in super cavitation or choked cavitation. Hence, it is important to select the proper cavitation number range and geometry of the cavitating device in order to obtain better degradation without the use of any external additives or catalysts.

3.3. Effect of frequency (ultrasonic cavitation)

In the case of ultrasonic cavitation, the frequency of the ultrasound is one of the most influential parameters and is essential while treating the wastewater. One of the interesting studies examining the degradation of Rh B using various ultrasonic reactor frequencies was conducted by Gogate et al. (2004) [96]. The frequency range employed to determine the change in dye concentration was 20 kHz–50 kHz, as well as the dual frequencies of 20 + 30, 20 + 50, 30 + 50, and the triple frequency of 20 + 30 + 50 kHz. Additionally, it was shown that the induction period lowers as the frequency of operation increases, such as 14 min for 20 kHz, 10 min for 30 kHz, and 6 min for the 50 kHz operation. Furthermore, the dual-frequency and triple-frequency operations did not include an induction period. The degree of degradation for the single-frequency operation over the course of the entire irradiation duration was said to be in the 20 > 30>50 kHz range. When compared to single frequency operation, the extent of degradation for dual and triple frequency operation was found to be greater. The combined operation for the 20 + 30 kHz operation resulted in a concentration change of 0.138 g/mL, whereas the individual operations for the 20 kHz operation and the 30 kHz operation yielded concentration changes of 0.043 g/mL and 0.1 g/mL, respectively. As a result, the combined operation's concentration decrease is slightly less than what would result from adding the individual operations. The other combination operations, 30 + 50, 20 + 50, and 20 + 30+50 kHz, also produced results that were comparable to or somewhat less degraded than the results of the individual operations (when added for the overall effect).

The rarefaction phase shortens as the irradiation frequency rises, which will have two effects: First, to maintain the same level of cavitation in the system, a higher amplitude (power) of irradiation will be required. In other words, if the same cavitational effects are to be maintained, more power is needed at higher frequencies. For instance, ten times more power is needed to cause water to cavitate at 400 kHz than at 20 kHz [97]. This explains why frequencies are often chosen between 20 and 40 kHz. Secondly, the generation of cavitation in liquids reduces when the ultrasonic frequency is raised towards the megahertz range. The simplest qualitative explanation is that the finite time necessary for the rarefaction cycle of the bubble occurs at a very high frequency, when the rarefaction (and compression) cycles are getting increasingly short. Additionally, it should be noted that transducers that operate at these high frequencies lack the mechanical ability to produce extremely high ultrasonic power [37].

Overall, it can be concluded that the ultrasonic horn gives higher degradation than the ultrasonic bath, even if the operating frequency is the same for both systems. When the energy is dissipated over a small volume, as in the case of horn, it provides more intensive cavitation, hence producing more intensive cavitation. On the other hand, it can be noted that the application of dual or triple frequency gives higher overall effectiveness compared to single frequency operation. However, this aspect must always be optimized in terms of energy conception.

3.4. Effect of power density (ultrasonic cavitation)

Ultrasonic power dissipation is a key element that influences the efficiency of dye degradation as well as the energy consumption and cost of treatment. When ultrasonic power is increased to its maximum value, the rate of degradation also increases due to an increase in the number of cavitation bubbles and collapse intensity, resulting in a larger formation of hydroxyl radicals. Furthermore, the turbulence caused by increasing the power density to the optimum improves the mixing intensity. The size of the created bubbles grows as power density increases. Nevertheless, a larger bubble size leads to a less dramatic bubble collapse, resulting in a slower rate of degradation. Furthermore, the larger quantum of cavitating bubbles scatters sound waves, resulting in less energy dissipation in the solution. To achieve optimal dye degradation, the optimum power density is unique to the reactor configuration. Indeed, the experimental results in the literature can be used to support the discussion. Aguilar et al. (2014) [98] studied the effect of power density from 100 to 500 W/L on the degradation of Rh B using ultrasounds at 20 kHz. It was reported that decolorization increased with a reduction in power densities due to the amount of energy dissipated per unit volume. Furthermore, maximum color degradation of Rh B was obtained at 300 W/L in 200 min of reaction time. In another study, Shivkumar and Pandit (2001) [99] reported that using the power density parameter instead of the power intensity parameter gives a clear idea of how much power is introduced into a given volume of solution. According to available reports, at a power intensity of 4.3 W/cm^2, the Rh B dye was degraded by 33% within 30 min, after that time its degradation significantly slowed down. As a result, the optimal power density at a level of 250–350 W/L ensures effective degradation with minimized costs of energy.

3.5. Effect of reaction vessel (ultrasonic cavitation)

When applying ultrasonic cavitation, it is quite exciting to observe the reactions that take place in the vessel, especially when the treatment is done on a scale that is between 0.1 and 1 L in volume. Based on these, Zhang et al. (2019) [100] investigated the degradation of Rh B using four different shapes of vessels under ultrasonic irradiation at 250 mL capacity. The three-neck bottle flask, round-bottom flask, beaker and conical flask were used with an initial concentration of Rh B of 10 ppm, 40 kHz (300W) and 500 rpm. It was reported that the three-neck bottom flask gives 98.06%, the round-bottom flask gives 94.58%, the conical flask gives 91.75% and the beaker gives 88.36% degradation of Rh B at 60 min of reaction time. The reason behind the maximum degradation of Rh B using a three-neck bottom flask rather than other shapes of vessels used in the investigation was reported due to the blocking and reflection of ultrasonic waves. Due to the flat bottoms of the conical flask and beaker, ultrasonic vibrations rapidly and inertly radiate the liquid. Uneven container surfaces harm the ultrasonic bath's standing wave. As a result, the sound field will be more evenly distributed. Thus, the energy that is produced by the ultrasonic bath can be utilized very effectively. The type of reaction vessel also affects the trends and should be taken into consideration while selecting the operating conditions.

Table 2
Degradation process optimization parameters based on reaction variables.

Type of Process	Variable	Specification	Operating parameter	Results	Reference
HC (Circular Venturi)/Rh B	Temperature	4 l, reciprocating pump, 1.1 kW, venturi,	30-40°C (4.90 bar, 10 ppm, 2.5 pH)	65% degradation at 40°C after 120 min	[68]
HC(Circular Venturi)/Rh B		4 L, centrifugal pump (3.0 kW), 3 cm depth of horn	16-60°C (Pressure 4 bar, pH 3, 10 ppm dye concen)	38.5% degradation at temperature of 30°C after 120 min	[70]
HC/Multi-orifice plate/Rh B		300L, Centrifugal pump (3 kW), 18 orifice holes (2 mm diameter)	13–40°C (0.3 g/L of CCl4, pH 3.0,3 bar)	83.02% degradation and 0.92 × 10-2 min-1 rate constants at temp of 22°C after 210 min	[71]
HC (Slit Venturi)/Rh 6G	pH	20 l, piston pump, 2.2 kW Slit venturi (α = 2.63)	2–12	Maximum decolorization of 32.06% at pH 10. Lower decolorization at acidic pH after 120 min	[69]
HC (Circular Venturi)/Rh B		4 l, reciprocating pump, 1.1 kW, venturi	2.5–11	Maximum degradation of 59.3% (TOC reduction 30%) at pH value of 2.5 after 120 min	[68]
Ultrasonic cavitation/ Rh 6G		2 L, US bath, 170W, 50 kHz	1.5–13.5 (120 min, 10 ppm dye concen.)	Maximum degradation at basic pH (11.5–12.5) than acidic pH (1.5–3.5) after 180 min	[104]
Ultrasonic/Rh B		250 mL, 20 kHz, 3 cm depth of horn	1–7 (10 ppm dye concen, 800 W)	42.03% degradation at pH of 3 after 100 min	[70]
HC(Circular Venturi)/Rh B		4 L, centrifugal pump (3.0 kW), 3 cm depth of horn	1–6 (4 bar, 10 ppm dye concen, 25°C)	38.7% degradation at pH of 3 after 120 min	[70]
HC/Multi-orifice plate/Rh B		300L, Centrifugal pump (3 kW), 18 orifice holes (2 mm diameter)	2.0–4.0 (0.3 g/L of CCl4, 10 ppm, 3 bar, temp 13°C)	96.42% degradation and 1.68 × 10-2 min-1 rate constants at pH of 2.0 after 210 min	[71]
Ultraviolet/Rh B		100 mL, 6W of UV lamp	1, 7 and 9 (H2O2 loading 1.67 mM, 10 μM, Temp 25°C)	73% degradation at pH of 7 in 30 min	[105]
UV/Rh 6G		500 mL, five of 30 W of UV lamp	2–10 (0.5 g/L ZnO, 25 ppm dye, 180 min)	Maximum degradation of 98% at pH of 10, 90% at pH of 8, 85% at pH of 4, 90% at pH of 8, 75% at pH of 2 in presence of ZnO	[106]
US and UV/Rh B and Rh 6G		2 L, US-50 kHz, 170 W, UV-11W	2.5–10.5 (180 min, 10 ppm)	Maximum degradation of Rh B (32%) and Rh 6G (52%) using US Maximum degradation of Rh B (25%) and Rh 6G (40%) using UV	[107]
HC (Slit Venturi)/Rh 6G	Initial concentration	6 L, piston pump, 2.2 kW Slit venturi (α = 2.63)	10–50 ppm	32.06% decolorization of Rh6G at initial concentration 10 ppm in 120 min	[69]
Ultrasonic cavitation/ Rh 6G		2 L, US bath, 170W, 50 kHz	10, 20 and 50 ppm (180 min, pH 12.5)	Maximum degradation 7.9% at 10 ppm after 180 min	[104]
Ultrasonic/Rh B		250 mL, 20 kHz, 3 cm depth of horn	5, 10 and 15 ppm 800 W	36.6% Degradation at 10 ppm after 90 min	[70]
Ultrasonic/Rh B		0.5 L, 35 kHz, 170 W	1–10 ppm, (Temp 25°C)	Maximum degradation at 5 ppm in 180 min	[74]
HC/Multi-orifice plate/Rh B		300L, Centrifugal pump (3 kW), 18 orifice holes (2 mm diameter)	5–20 ppm (0.3 g/L of CCl4, pH 3.0,6 bar, 13°C)	85.02% degradation at 10 ppm after 210 min	[71]
Ultraviolet/Rh B		100 mL, 6W of UV lamp	2.5–20 μM (H2O2 loading 1.67 mM, Temp 25°C)	96% degradation at 2.5 μM in 30 min	[105]
UV/Rh 6G		500 mL, five of 30 W of UV lamp	5–200 mg/L (0.5 g/L ZnO, 25 ppm dye,pH 10, 180 min)	Complete decolorization at 25 ppm after 240 min	[106]
HC(circular venturi)/Rh B		4 L, centrifugal pump (3.0 kW), 3 cm depth of horn	6–18 ppm (Pressure 4 bar, pH 3, 25°C)	37.3% degradation at concentration of 10 after 120 min	[70]
US and UV/Rh B and Rh 6G		2 L, US-50 kHz, 170 W, UV-11W	5–50 ppm (pH 2.5,180 min)	Maximum degradation of Rh B (20%) and Rh 6G (29%) at 10 ppm using US after 180 min Maximum degradation of Rh B (18%) and Rh 6G (24%) at 10 ppm using UV after 180 min	[107]

3.6. Effect of type of UV light

It is interesting to have an understanding of the efficacy of different types of UV lamps on the degradation of contaminants in wastewater solutions. Aliabadi and Sagharigar (2011) [101] reported that lamps with shorter wavelengths lead to faster degradation. The kinetic degradation rate constant was in the order of UVC (0.051 min^{-1}) > UVA black light (0.035 min^{-1}) > UVA black light blue (0.026 min^{-1}) > day light (0.016 min^{-1})>UV-LED (0.005 min^{-1}). The UVC lamp was reported to show significant enhancement in the degradation of Rh B due to the maximum illumination intensity. In another study [102], it was also reported that the complete removal of Rh B at 250 W of UV light took 50 min, whereas 99.42% decolorization of Rh B was obtained using 80W of visible light after 90 min in the presence of a ZIF-8/$BiFeO_3$ catalyst of 1 g/L. Similar results were also reported by Hiremath et al. (2017) [64], stating that UV light gives maximum degradation (70%) of Rh B as compared to visible light (40%) in the presence of TiO_2 catalysts (150 mg). Bhaskar et al. (2015) [103] also reported the maximum degradation of Rh 6G of 96.5% and COD removal of 92% at the optimal combined loading conditions of TiO_2 (3 g/L) and $CuSO_4$ (1.5 g/L) using solar irradiation.

Thus, it can be advisable to use UVC lamps as a good source of illumination compared to other UV sources and in tropical countries, sunlight is the best option if it is available in abundant form.

4. Optimization of process parameters

It is always beneficial to obtain the efficacy of a reaction based on optimizing the reaction variables such as initial dye concentration, pH, reaction volume, temperature, stirring speed etc. After reviewing the literature on optimized parameters based on reaction variables using cavitational reactors, and photocatalytic reactors for Rh dyes, the most significant operational factors that impact the overall degradation efficiency of the processes are described in Table 2. Below, an analysis of the influence of the most important factors is discussed.

4.1. Effect of temperature

The cavitation and/or photocatalysis processes both depend on the operating temperature, which has a significant impact on final degradation effectiveness. The solution's physical and chemical characteristics as well as the intensity of the collapse are mostly affected by the operating temperature. Zhang et al. (2014) [108] investigated the effect of initial temperature on Rh B degradation using hydrodynamic cavitation (multi-orifice). It was reported that the degradation of Rh B increased with an increase in the initial temperature for the first 60 min of treatment. However, with a further increase in treatment time to 210 min, the trends of degradation of Rh B were different. The maximum degradation of Rh B of 83.02% was obtained at 22 °C with a rate constant of 0.92×10^{-2} min^{-1} and the lower degradation was reported at a higher temperature of 40°C with a rate constant of 0.70×10^{-2} min^{-1}. Similar results were also reported by Mishra and Gogate (2010) [109] on the temperature effect on the degradation of Rh B using hydrodynamic cavitation (venturi). It was demonstrated that with an increase in temperature from 30 to 40 °C, a corresponding increase in the extent of degradation from 56% to 65% was observed. Chen et al. (2016) [110] investigated the effect of temperature on Rh B degradation using ultrasonic irradiation (60 kHz) in the presence of catalyst -Bi_2O_3 particles (1 g/L). The author also reported that the degradation increased from 20 °C (75%) to 40 °C (95.6%) but decreased with a further increase in temperature up to 50 °C in 90 min of reaction time. Due to favorable kinetics, degradation should increase with temperature. The optimal temperature relies on reactor design (jacketed or non-jacketed), hydroxyl radical reaction rate, cavitating circumstances, and Rh dyes [111–113], increasing temperature increases the number of nuclei, cavity development, and pollution degradation to the optimum limit. Beyond the ideal temperature, a significant number of cavities are formed, filled with more vapor, reducing the intensity of cavitation and decreasing the degrading effectiveness of compounds. It is known that during the lowering of the surface tension of the liquid along with increased temperature, the energy of bubble collapses decreases leading to less effective degradation [57]. Importantly, the cavitation number should be controlled and fixed, while the temperature changes as it changes the density of the fluid. Thus, under different temperature and fixed flow rate the cavitation number will be a bit different.

Barka et al. (2008) [114] investigated the effect of temperature on the degradation of Rh B using UV irradiation with a TiO_2 coated non-woven paper. It was reported that the rate of degradation of Rh B increased with an increase in temperature (20–40 °C). This increase in degradation was attributed to higher adsorption capacity of the catalyst. Additionally, increased temperature leads to higher adsorption of Rhodamine B and it also makes the reaction more competitive with lower rate of e^- - h + recombination [115], but it also increases the amount of Rh B that is adsorbed on the surface of the photocatalyst. The rate of desorption of the products generated is a limiting factor in the reaction when it is working at a low temperature since it is a slower process than the degradation on the surface and the adsorption of the reactants.

Overall, in general, lower operating temperature values typically from 30 to 40 °C are proposed to be more effective for applications where cavitational collapse and free oxidizing radicals are the major factors responsible for degradation.

4.2. Effect of initial pH of the solution

Owing to significance of pH in determining the efficacy of contaminant degradation various studies reported optimization of the degradation process along with the impact of the initial pH of the solution on the extent of degradation. Some of the key findings were as follows: Mishra and Gogate (2010) [109] investigated the effect of pH on the degradation of Rh B dye using hydrodynamic cavitation (venturi 2 mm in diameter). The range of pH was 2.5–11. A maximum degradation of 59.3% and 30% TOC removal were found

under acidic conditions, such as pH 2.5. It was also reported that a considerably lower extent of degradation of Rh B was obtained at alkaline and neutral pH. Ye et al. (2021) [70] investigated the degradation of Rh B using a circular venturi based cavitating device via hydrodynamic cavitation. The range of solution pH was used from 1 to 6. It was reported that the extent of degradation of Rh B was higher at low pH than at higher pH. The authors also reported that 38.7% degradation was obtained at a solution pH of 3 and a 19.2% of degradation at a solution pH of 6 in 120 min of reaction time. Similar results were reported by several other papers [116–120]. The authors reported that the generation of hydroxyl radicals and its oxidation capacity are higher when exposed to acidic conditions; hence, the obtained degradation of Rh B was higher. In contrast, the results that were obtained showed divergent trends when the Rh 6G dye was degraded under the influence of pH. In 2013, Banerjee et al. (2013) [121] investigated the effects of the solution's initial pH on the decolorization of Rh 6G using ultrasonic irradiation (170 W, 50 kHz). According to the investigation, the experiments revealed that under more acidic conditions (pH 1.5–3.5), ultrasonic decolorization rates are lower than those at higher operating pH (pH 11.5–12.5). It was also reported that the decolorization rate increases under strong alkaline conditions, from pH 9.5 to 12.5; at pH 12.5, the maximum extent of decolorization was achieved. According to the authors, Rh 6G exists in two main forms: ionic ($Rh\ 6G^{+}$) and non-ionic ($Rh\ 6G^{-}$), which can be used to explain the reported results. Due to the dye's non-ionic nature, a greater dye quantum is anticipated under fundamental circumstances close to the site of cavity collapse, resulting in quicker rates of degradation. The hydrophilic nature of the pigment could also contribute to the faster rate of degradation when exposed to extremely basic conditions (pH 10) as opposed to the hydrophobic quality in an acidic environment.

The effects of pH on photocatalytic oxidation rates are complicated, and the observed effects are typically influenced by both the pollutant type and the semiconductor's point of zero charge (PZC), or more particularly, the electrostatic attraction between the surface of the catalyst and the pollutant [122]. The pollutant will adsorb most strongly near the catalyst's PZC, which will result in the highest degradation rates. Due to the fact that effluent containing dyes is produced in actual industrial operations at a variety of pH levels depending on the processing parameters, it is essential to evaluate how pH affects the effectiveness of degradation. According to Patil et al. (2015) [123], solution pH was observed to have an impact on the degradation of Rh 6G in a photocatalytic reactor. In this experiment, a ZnO-montmorillonite nano-composite catalyst at 1 g/L was utilized, with a pH range of 2–9. When Rh 6G's solution pH was 3, the maximum degradation rate was 98.1%; however, as the pH changed to basic, i.e., pH 9, the degradation percentage (91.4%) decreased as well, revealing the applicability of this catalyst in a wide pH range.

Overall, it was concluded that the effective degradation Rh B favors acidic conditions, whereas Rh 6G favors basic pH conditions when the cavitation process is used; otherwise, acidic conditions are suitable for significant degradation of both Rh dyes.

4.3. Effect of stirring speed

Stirring speed is one of the crucial parameters in a photocatalytic batch reactor. However, in the case of an ultrasonic horn, it may be advantageous to keep catalysts in suspension form but is not necessary to employ as ultrasound provides micro-level mixing. Zhang et al. (2019) [100] investigated the impact of mechanical mixing speed on Rh B degradation rate using an ultrasonic bath at 40 kHz. The Rh B degradation was studied at speeds of zero rpm to 900 rpm with a dye concentration of 10 ppm in three necked reaction vessels. When the rotating speed was more than 300 rpm, it was claimed that the degradation rate of Rh B remained almost constant. Therefore, the authors performed another set of experiments by changing the range of stirring speed from 500 to 1100 rpm to explore the ideal mixing speed for degradation. Within 45 min of reaction time, the degradation of Rh B was 94.98%, 97.60%, 89.16%, and 89.82% at stirring speeds of 500, 700, 900, and 1100 rpm, respectively. It may be due to the combination of high-speed stirring and ultrasonication that may enhance a high concentration of bubbles. Under the influence of an ultrasonic sound field, the bubble will enlarge and compress, which can help to induce cavitation more easily and quickly. Agitation also improved mass transfer efficiency and solution vortex. The author also suggests that fast stirring rates are not required for efficient Rh B decomposition. The effect of stirring speed on degradation of Rh B using a photocatalytic reactor was studied by Madjene et al. (2019) [124] and it was reported that 100% COD removal was obtained when stirring speed was 600 rpm, while 96.79% COD removal was reported when stirring speed was 575 rpm in the presence of ZnO catalysts. The rate of degradation is significantly influenced by the stirring speed due to the aggregation and dispersion properties of catalyst particles.

Thus, in general, the high stirring speed keeps the catalysts suspended, resulting in rapid mass transfer diffusion and improved mixing characteristics, which results in significant degradation of Rh dyes. In the case of a sole cavitation process, the agitation is not so important as ultrasounds or high linear velocity (HC) provide enough microcirculations or turbulence (respectively) to maintain mass transfer at the needed level.

4.4. Effect of initial dye concentration

According to the literature, the extent of degradation depends on hydroxyl radical production and the availability of contaminants for interaction. As a result, the effect of initial Rh dye concentration is a key optimization parameter for achieving more degradation. In accordance with this, Ye et al. (2021) [70] investigated the effect of initial Rh B concentration using a venturi (2 mm in diameter) as a cavitating device via hydrodynamic cavitation at a capacity of 4L. The initial Rh B concentration varied from 6 to 18 ppm with a fixed reaction condition. It was found that with an increase in the initial dye concentration up to the optimum limit, the degradation of Rh B increases. However, with a further increase in initial Rh B concentration, the degradation of Rh B decreases. It was reported that the maximum degradation of Rh B of 37.3% was obtained at 10 ppm of Rh B and the minimum degradation of 16% was obtained at 6 ppm of Rh B concentration. Similar results were also reported by Yi et al. (2018) [80], who reported an increase in the degradation rate from 0.00117 to 0.00136 min^{-1} when the initial concentration of Rh B varied from 20 to 40 $\mu mol\ L^{-1}$. Identical findings were also reported

by Behnajady et al. (2007) [74] while investigating the degradation of Rh B using an ultrasonic bath of 35 kHz and output power of 170 W. The range of initial dye concentration was from 1 to 10 ppm, whereas it was reported that due to the increased concentration of intermediates generated and the limited interfacial region, it was claimed that the decolorization rate falls with an increase in initial Rh B concentration. The maximum degradation of Rh B was obtained at 5 ppm. The quantity of hydroxyl radicals near the surface of collapsing bubbles is extremely high [125]. Additionally, an increase in the initial concentration leads to an increase in the degradation of pollutants, increasing the probability of reaction between pollutants and oxidizing radicals. The quantity of hydroxyl radicals created by cavitational events is insufficient to compete with the overall number of pollutant molecules in a high-content pollutant

Table 3
Degradation process optimization parameters based on catalytic processes.

Type of Process	Variable	Specification	Operating parameter	Results	Reference
Ultrasonic cavitation/ Rh 6G	Titanium dioxide	2 L, US bath, 170W, 50 kHz	1.5–4.5 g/L (pH 12.5; dye concen.10 ppm, 180 min)	51.2% degradation at 4.0 g/L	[128]
Ultrasonic cavitation + Ultraviolet irradiation/Rh 6G		2 L, US bath, 170W, 50 kHz 9 W of UV lamp	1.5–4.5 g/L (pH 12.5; dye concen.10 ppm, 180 min)	51.2% (US) 28.9% (UV) 63.3% (US + UV) degradation at 4 g/L	[128]
Solar/Rh 6G		2 L, solar	1.5–4.5 g/L (pH 12.5; dye concen.10 ppm, 180 min)	72.3% degradation at 3 g/L	[103]
Ultraviolet/Rh B		250 mL, 26W UV lamps	0.4–2.4 g/L (5 ppm, 2 pH, 15 min)	Degradation increased from 41.06% to 75.06% for 0.4–1.6 g/L of TiO_2 and then decreased	[7]
US and UV/Rh B and Rh 6G		2 L, US-50 kHz, 170 W, UV-11W	0.1–0.4 g/L (pH 2.5, 10 ppm, 180 min)	Maximum degradation of Rh B (85%) and Rh 6G (81%) using US Maximum degradation of Rh B (71%) and Rh 6G (62%) using UV	[107]
HC (square venturi) Rh B	Fe^{3+} -doped Titanium dioxide	5L, Self-priming pump (2.2 kW)	0.05:1.0 M ratio of Fe: Ti (at 700 °C for 3.0 h and at 550 °C for 5.0 h),	91.11% degradation Fe + TiO_2 (0.05:1.00 M ratio of Fe:TiO_2 at 550 °C for 3.0 h) whereas 58.32% HC alone after 150 min	[51]
Ultrasonic/Rh B	Aluminum oxide	200 mL, 24 kHz,	60 ppm	8.25×10^{-3} min^{-1} for H2O2 +Al_2O_3+ US; 1.87×10^{-3} min^{-1} for H_2O_2 +Al_2O_3	[7]
Ultrasonic/Rh B	Iron oxide	200 mL, 24 kHz,	60 ppm	2.97×10^{-2} min^{-1} for H_2O_2 +FeO + US; 7.39×10^{-3} min^{-1} for H_2O_2 +FeO	[7]
Ultrasonic cavitation/ Rh 6G	Copper oxide	2 L, US bath, 170W, 50 kHz	1.5–4.5 g/L (pH 12.5; dye concen.10 ppm, 180 min)	52.8% degradation at 1.5 g/L	[128]
Ultrasonic cavitation + Ultraviolet irradiation/Rh 6G		2 L, US bath, 170W, 50 kHz 9 W of UV lamp	1.5–4.5 g/L (pH 12.5; dye concen.10 ppm, 180 min)	52.8% (US) 26.4% (UV) 60.8% (US + UV) degradation at 1.5 g/L	[128]
Solar/Rh 6G		2 L, solar	1.5–4.5 g/L (pH 12.5; dye concen.10 ppm, 180 min)	30.2% degradation at 1.5 g/L	[103]
Solar/Rh 6G	Calcium oxide	2 L, solar	1.5–4.5 g/L (pH 12.5; dye concen.10 ppm, 180 min)	20.6% degradation at 3 g/L	[103]
UV/Rh 6G	ZnO	500 mL, five of 30 W of UV lamp	0.25–2.0 g/L ZnO (25 ppm dye,pH 5.97)	Maximum degradation of 95% at 0.5 g/L ZnO	[106]
UV/Rh 6G		UV W, 300 mL ZnO prepared by zinc nitrate precipitation in urea medium	pH 8.5 ZnO 0.3 g/L	74.70% dye removal and 67.10% for 30 ppm and 50 dye concentration in 90 min, respectively	[129]
HC (Circular Venturi)/ Rh B	Fenton	4 l, reciprocating pump, 1.1 kW, venturi	eSO_4:H_2O_2 in the ratio of 1:5	99.9% degradation of with TOC degradation of 57%.	[68]
US and UV/Rh B and Rh 6G		2 L, US-50 kHz, 170 W, UV-11W	FeSO4.7H2O loading of .1–0.4 g/L (H2O2 fixed 0.2 g/L) (pH 2.5, 10 ppm, 180 min)	Maximum degradation of Rh B (83%) and Rh 6G (82%) using US Maximum degradation of Rh B (67%) and Rh 6G (62%) using UV	[107]
Ultrasonic/Rh B	Iron oxide	200 mL, 24 kHz,	60 ppm	2.97×10^{-2} min^{-1} for H_2O_2 +FeO + US; 7.39×10^{-3} min^{-1} for H_2O_2 +FeO	[7]

mixture. As a result, as the initial concentration increases, the degradation rate of the Rh dye decreases. As an example, Kansal et al. (2007) [126] found that the initial dye concentration had an impact on Rh 6G decolorization in a photocatalytic reactor. It was reported that when the dye concentration was increased, the rate of photo decolorization reduced, indicating that other factor like the catalyst dose or the time span for complete removal are also important in complete removal. It was also reported that for dye solutions of 5 and 10 ppm, nearly 100% degradation took place within 30 and 60 min, respectively, and for dye solutions of 25 ppm, almost total degradation occurred but the required time was 3 h. Degradation of the dye solution containing 50 ppm was 75% in 4 h, and it further declined as dye concentration was increased. It is essential to remember that the number of moles degraded per unit of energy supplied may or may not be lower at higher concentrations and that the adverse effects of increased power requirements for treating large quantities of effluent must also be considered. The Langmuir-Hinshelwood model type can be used to associate the observed rates with the pollutant's initial concentration [98,127], but the model's parameters will be highly dependent on the effluent's composition as well as other reactor operating variables for photocatalytic processes.

Summarizing, it is clear that the concentration of pollutant effectively degraded directly relates to the amount of formed radical species. In the case of sole cavitation-based processes, effective degradation in a reasonable time of maximum 2 h takes place for up to 10 ppm concentration levels, while for photocatalytic processes this level reaches even 50 ppms. In both cases degradation of higher doses of pollutants is possible but demands a longer treatment time. Generally, these conclusions are positive as typically, in real-world scenarios, the concentration level of pollutants is of single ppm levels or lower, so these technologies have a high potential for routine application.

5. Intensification techniques

The "process intensification" is a highly innovative concept applied to improving the productivity of chemical process plants using a sustainable approach. Process intensification can be achieved by intensifying of mass transfer, increasing the rates of reaction by using various catalysts (TiO_2, MnO_2, starch, ZnO etc.), external oxidants (H_2O_2, air, O_3, persulfate etc.) and additives (NaCl, surfactants etc.) or by combining both catalysts and additives based on cavitation or photolysis approaches. The following sections relate to this aspect in detail. Table 3 lists the most important operational conditions that have an impact on the processes' total degradation efficiency.

5.1. Effect of catalysts

In this section, the effects of the catalyst and catalyst loading have been evaluated. TiO_2 [63,130–134], MnO_2 [135,136], CuO [137–139], ZnO [124,140–143], Ag nanoparticles [12], Bi_2O_3 [110,144], C_3N_4/ZnFe [145] etc. are some of the commonly used photocatalysts documented in the literature for the treatment of wastewater. The catalyst concentration should be optimized, as employing a larger dose limits the quantity of photo-energy that can be transported in the medium due to the increased turbidity. Lab-scale studies are necessary to find the optimal value if proper data are not available in the existing literature, especially for similar operating conditions. The type and concentration of pollutants and rate of free radical formation will have a significant impact on the optimal value (depending upon the operating conditions of the reactor). As a result, many researchers used either different individual catalysts or combinations of doped or immobilized catalysts or catalyst composites to increase the rate of degradation of the Rh family.

Li et al. (2020) [146] investigated the use of the photocatalyst titanium dioxide (TiO_2) on the degradation of Rh B using hydrodynamic cavitation. The square venturi (LS) tube with a side length of 1.77 mm and a corresponding cross section area of 3.14 mm^2 was used as a cavitating device. The TiO_2 concentration of 0.5 g/L was used for the degradation of Rh B at the 10-ppm level. An extent of degradation of 58.3% in 150 min was obtained when hydrodynamic cavitation was used as the sole process, HC with Fe^{3+} doped TiO_2 achieved a degradation extent of 91.1%. Chen et al. (2023) [147] reported that the degradation of ciprofloxacin using hydrodynamic cavitation coupled with TiO_2 catalysts decreased from 55.7% to 27.4% when the pH of the solution increased from 7 to 3. According to the author, this reason was brought on by the corrosion and decomposition of catalysts in acidic environments. Additionally, the degradation was slowed down by the electrostatic attraction between the ciprofloxacin molecule and the photocatalyst surface.

Bokhale et al. (2014) [148] studied the effect of a cupric oxide catalyst on the ultrasonic degradation of Rh 6G at a frequency of 50 kHz and a power output of 170 W. Within 3 h of the reaction, it was reported that 52.8% of Rh 6G was degraded at a catalyst loading of 4.5 g/L. Combining this process with ultraviolet light (11 W) gave a slight improvement in degradation – up to 60.8%. In another study, nano-sized zinc oxide (ZnO) was used for the degradation of acid red B and Rh B under ultrasonic irradiation [149]. It was reported that sole acoustic cavitation (US bath of 40 kHz and output power of 50 W) gave 8.2% degradation, while the sonocatalytic process allowed to remove 39.1% of Rh B in 60 min of reaction time. It was also reported that maximum degradation was obtained at pH 13 with a catalyst dose of 1.5 g/L. Also, pure TiO_2 photocatalysts were studied for Rh B degradation [150]. Interestingly, a 95.48% degradation was obtained in only 40 min of treatment. It was explained that the introduction of heterogeneous surfaces results in an increase in the number of nuclei, and that the amount of catalyst also increases the extent of interfacial cavitation. In this case, dual roles as photocatalyst and sonocatalyst can be assigned. The catalyst's surface area is increased during the ultrasonic process by surface pitting and fragmentation. Additionally, due to the turbulence produced by the cavitating conditions and the improved mass transfer between the two phases, acoustic and hydrodynamic cavitation leave the catalyst's surface clean during the treatment. Utilizing an optimal loading is crucial because the accessible surface and energy flow are both affected by the catalyst loading, which has a negative impact on the degradation. Based on the literature, it comes to know that there was no study reporting the reusability of metal catalysts (TiO_2, CuO etc) for the treatment of wastewater. Thus, it is important to note here that future research should also include these aspects related to recycling and reusing the metal catalysts and finding their stability for the degradation of pollutants. It is crucial to evaluate if the

Table 4
Degradation process optimization parameters based on additional external oxidants.

Type of Process	Additional external oxidants	Specification	Operating parameter	Results	Reference
HC (Slit Venturi)/Rh 6G	Hydrogen peroxide	6 L, piston pump, 2.2 kW Slit venturi (α = 2.63)	1:10–1:50 dye: H_2O_2	53.72% decolorization with 21.6 × 10^{-3} min^{-1}	[69]
HC (Circular Venturi)/Rh B		4 L, reciprocating pump, 1.1 kW, venturi,	10 mg/L to 200 mg/L	Degradation of Rh B from 59.3% using only venturi to 99.9% in the presence of 200 mg L^{-1} H_2O_2 with TOC reduction of 55%.	[69]
Ultrasonic cavitation/Rh 6G		2 L, US bath, 170W, 50 kHz	0.2–3 g/L (120 min, 10 ppm dye concen., pH 12.5)	77.8% decolorization with 1.25 × 10^{-2} min^{-1} at 1 g/L of H_2O_2	[104]
Ultrasonic/Rh B		250 mL, 20 kHz, 3 cm depth of horn	0.15–0.75% (v/v) (10 ppm dye concen, pH 3, 800 W)	84.06% degradation at 0.6% H_2O_2 after 100 min	[70]
Ultraviolet/Rh B		250 mL, 26W UV lamps	0.1–1 mL/L (5 ppm, 2 pH, 30 min)	Degradation increased from 81.62% to 94.46% for 0.1–0.4 mL of H_2O_2 and then decreased	[7]
Ultraviolet/Rh 6G		5 μM, UV lamp (8W) White lamp (8W)	5 μM H2O2 (21 °C, 10 TiO2 supported on Rasching rings)	60.1% degradation (1.9 × 10-3 min-1) using UV light and 51.6% with rate constant (1.7 × 10-3 min-1) using white light	[151]
Solar/Rh 6G	Salts	2 L, solar	1.5–4.5 g/L (pH 12.5; dye concen.10 ppm, 180 min)	26.7% (1.5 g/L of $FeSO_4$) 32.5% (1.5 g/of Na_2CO_3) 30.7% (1.5 g/L of $CuSO_4$) degradation	[103]
Ultraviolet/Rh B		100 mL, 6W of UV lamp	chloride, nitrate, sulfate and phosphate ions (0.5 mh/mL) (H2O2 loading 1.67 mM, 7 pH, 10 μM, Temp 25°C)	69%, 49%, 28% and 44% degradation using chloride, nitrate, sulfate and phosphate ions, resp.	[105]
Ultrasonic/Rh B		0.5 L, 35 kHz, 170 W	0.5–2.5 g/L (5 ppm, Temp 25°C)	Maximum degradation at 0.625 g/L	[74]
US and UV/Rh B and Rh 6G		2 L, US-50 kHz, 170 W, UV-11W	0.1–0.4 g/L (pH 2.5,10 ppm, 180 min)	Maximum degradation of Rh B (64%) and Rh 6G (69%) using US Maximum degradation of Rh B (56%) and Rh 6G (60%) using UV	[107]
HC (Slit Venturi)/Rh 6G	t-butanol	20 L, piston pump, 2.2 kW Slit venturi (α = 2.63)	1 mL/L (10 ppm initial concentration slit venturi)	22% decolorization in 120 min	[69]
Ultrasonic cavitation/Rh 6G		2 L, US bath, 170W, 50 kHz	1.5–4.5 mL/L (pH 12.5; dye concen.10 ppm)	26.0% degradation at 1.5 mL/L	[128]
Ultrasonic cavitation + Ultraviolet irradiation/Rh 6G		2 L, US bath, 170W, 50 kHz 9 W of UV lamp	1.5–4.5 mL/L (pH 12.5; dye concen.10 ppm)	26.0% (US) 37.2% (UV) 12.3% (US + UV) degradation at 1.5 mL/L	[128]
Solar/Rh 6G		2 L, solar	1.5–4.5 mL/L (pH 12.5; dye concen.10 ppm, 180 min)	25.4% degradation at 1.5 mL/L	[103]
Ultrasonic cavitation/Rh 6G	methanol	2 L, US bath, 170W, 50 kHz	1.5–4.5 mL/L (pH 12.5; dye concen.10 ppm)	23.7% degradation at 4.5 mL/L	[128]
Solar/Rh 6G		2 L, solar	1.5–4.5 mL/L (pH 12.5; dye concen.10 ppm, 180 min)	20.1% degradation at 1.5 mL/L	[103]
Ultrasonic cavitation + Ultraviolet irradiation/Rh 6G		2 L, US bath, 170W, 50 kHz 9 W of UV lamp	1.5–4.5 mL/L (pH 12.5; dye concen.10 ppm)	23.7% (US) 46.9% (UV) 34.0% (US + UV) degradation at 4.5 mL/L	[128]
HC (Slit Venturi)/Rh 6G	Ozone	6 L, piston pump, 2.2 kW Slit venturi (α = 2.63)	1–7 g/h slit venturi	Complete decolorization in 10 min at 3 g/h, however, TOC reduction was 73.19%	[69]
Ultrasonic cavitation/RH 6G	CCl4	2 L, US bath, 170W, 50 kHz	0.5–1 g/L (120 min, 10 ppm dye concen., pH 12.5)	22.0% decolorization with 1.82 × 10^{-2} min^{-1} at 1 g/L of CCl4	[104]
HC (Circular Venturi)/Rh B		4 l, reciprocating pump, 1.1 kW, venturi	1 g/L (10 ppm)	82% degradation and 34% TOC in presence of CCl4 (59.3% degradation and 30% TOC w/o CCl4)	[68]

(*continued on next page*)

Table 4 (*continued*)

Type of Process	Additional external oxidants	Specification	Operating parameter	Results	Reference
HC/Multi-orifice plate/Rh B		300L, Centrifugal pump (3 kW), 18 orifice holes (2 mm diameter)	0.3–1.2 g/L (pH 3.0, 10 ppm, 3 bar, temp 13°C)	80.38% degradation and 0.81 × 10-2 min-1 rate constants at 1.2 g/L CCl4 after 210 min (70.78% in absence of CCl4)	[71]
UV/Rh B	Potassium persulfate ($K_2S_2O_8$)	XPA-7 merry-go-round photochemical reactor, 300W mercury lamp, natural pH	Natural pH, Rh B concentration 0.2 mM	35% degradation using UV while 85% degradation at 0.2 mM of $K_2S_2O_8$ (0.2 mM) at 60 min.	[157]
Ultrasonic cavitation/Rh 6G	Air	2 L, US bath, 170W, 50 kHz	31.25 cm3/s (120 min, 10 ppm dye concen., pH 12.5)	22.8% decolorization with 2.3 × 10^{-3} min^{-1} with air	[104]
Ultrasonic/Rh B		250 mL, 35 kHz 300W,	25, 40, 60 and 80 kHz (20 ppm, Temp 24°C)	Maximum degradation of 98.39% and 95.388% with and without air after 40 min.	[73]
Ultrasonic cavitation + Ultraviolet irradiation/Rh 6G	CuO + alcohol	2 L, US bath, 170W, 50 kHz 9 W of UV lamp	pH 12.5; dye concen.10 ppm	70.07% (US+1.5 g/L CuO+ 1.5 mL/L butanol) 67.0% (US+1.5 g/L CuO+ 4.5 mL/L methanol)	[128]
US and UV/Rh B and Rh 6G	NaCl + TiO_2	2 L, US-50 kHz, 170 W, UV-11W	NaCl of 0.1–0.4 g/L (TiO2 fixed 0.3 g/L) (pH 2.5, 10 ppm, 180 min)	Maximum degradation of Rh B (91%) and Rh 6G (91%) using US Maximum degradation of Rh B (56%) and Rh 6G (64%) using UV	[107]
Solar/Rh 6G	TiO_2 + $CuSO_4$	2 L, solar	1.5–4.5 g/L (pH 12.5; dye concen.10 ppm, 180 min)	96.5% (3 g/L TiO_2+1.5 g/L $CuSO_4$) 89.4% (1.5 g/L CuO+1.5 g/L $CuSO_4$) 79% (3 g/L CaO+1.5 g/L $FeSO_4$) degradation	[103]

developed catalyst is really useful in real case scenario, where stability is expected over several treatment cycles. The sonophotocatalytic oxidation process can have a synergistic effect on the breakdown of Rh dyes. Due to the huge quantity of hydroxyl radicals that are available and the increased catalytic activity at the catalyst surface in the combination approach for degradation, acoustic cavitation and photocatalysis together can lead to a greater rate of degradation of Rh dyes.

An interesting advancement in the field of process intensification was proposed by Pino et al. (2020) [151] by TiO_2 immobilization on Raschig rings. The degradation process of Rh 6G was aided by UV-VIS light (8 W). A 91% degradation was obtained for this approach. In a subsequent work, a cotton fabric infused with TiO_2 nanoparticles was also studied also for Rh 6G [152]. It was proven that combining photocatalytic process with ultrasounds allowed for 60% degradation in 120 min. Importantly, it was claimed that ultrasounds allow for effective degradation of Rh 6G, both adsorbed and remaining in the bulk solution. In another study, a ZnO catalyst was allowed to degrade 100% of Rh 6G in 8 h using a photocatalytic (UV) process [153].

Kansal et al. (2007) [126], systematically compared several semiconductor-based catalysts in one study for Rh 6G in a photocatalytic process. A TiO_2, SnO_2, ZnO, ZnS and CdS were evaluated. It was concluded, that the ZnO, and TiO_2, had better photocatalytic activity comparing to other catalysts. The maximum Rh 6G degradation of 98% was obtained for 3 h at a basic pH of 10.

In work of Lops et al. (2019) [154], a ZnO micro-and nanomaterial-based sonophotocatalytic method is suggested to effectively clean polluted waters from industrial dyes. The sonodegradation of Rhodamine B (Rh B) under ultrasonic irradiation was investigated for five types of zinc oxide (ZnO), namely micro-and nano-structures, including Desert Roses (DRs), Multipods (MPs), Microwires (MWs), Nanoparticles (NPs), and Nanowires (NWs). It was reported that sonocatalytic performance of the DRs micro particles (2 μm) gave best results (Rh B was completely degraded in 180 min), as it produced the most OH radicals when exposed to ultrasonic irradiation. It was also reported that combining ultrasounds and sunlight in the presence of DRs micro particles, has a lot of potential and can serve as a starting point for further research into the effective removal of organic dyes from wastewater.

Mishra and Gogate [109], also studied the effect of $FeSO_4$:H_2O_2 in a ratio of 1:5 for a 10-ppm initial concentration of Rh B using HC. It was reported that 99.9% Rh B degradation and 57% TOC removal were obtained using a 1:5 $FeSO_4$:H_2O_2 ratio. Akram et al. (2016) [155] studied the degradation of Rh B using an ultrasonic bath and horn using the Fenton process. The Fenton process ($FeSO_4$ concen. 1.79 × 10^{-2} mol/L, H_2O_2 dose of 9.795 mM) was investigated at 0.2 kg/M^3 and 0.5 kg/M^3 of dye concentration using an ultrasonic horn and bath at a pH of 3. It was reported that the US horn was more effective than the US bath. It was also reported that when using Fenton reagent alone at a higher initial dye concentration of 0.5 kg/m^3, maximum degradation of 73.68% was obtained; however, when using ultrasound and Fenton reagent together, maximum degradation of 92.39% for bath-type and 93.85% for horn-type sonicators was achieved. The COD removal of 30.66% and 32.91% was reported using an ultrasonic bath and horn in 15 min of reaction time. Hou et al. (2011) [156] studied the degradation of Rh B using advanced oxidation processes based on heterogeneous zero valent iron (ZVI) (Fe powder as catalyst) in the Fenton process. It was reported that the effect of ZVI and H_2O_2 at pH 4.0 provides complete degradation of Rh B at 1.0 g/L of Fe (0) and 2.0 mM of H_2O_2 in 20 min of treatment time. The other combinations of air, nitrogen and isopropanol were also investigated, but the degradation obtained was not more than 60%.

Rahmani et al. (2022) [27] studied photo-Fenton-PAA and Fenton-Peracetic Acid (PAA) processes for removal of the Rh B dye from aqueous solutions. The outcomes demonstrated that Rh B removal effectiveness was enhanced by lowering pH (in 3–9 range) and dye

concentration (in 25–500 mg/L range). Fenton's PAA process revealed to have a Rh B removal efficiency of 99.9% during 10 min of treatment. In comparison, this amount of dye might be eliminated in just 5 min using the photo-Fenton PAA technique. The synergistic effect of the photo-Fenton PAA process in the presence of UV is responsible for the system's great performance in a short period of time. The weak O-OH bond in PAA, allows easy activation of this chemical to produce high quantities of hydroxyl radicals for effective degradation of target contaminants. Additionally, the iron cation in solution forms a complex with Rh B, and this dye-iron complex then interacts with PAA to increase the removal effectiveness.

In general, for effective degradation of Rh dyes, it is important to select the appropriate type of catalysts in order to improve the effectiveness of degradation to an optimal level. The use of process intensification characteristics such as the addition of solid particles such as TiO_2, CuO, and others gives either extra nuclei for cavitation phenomena or active surface sites for oxidation reaction, resulting in net chemical and physical consequences. It can be also noted here that the complete degradation of Rh dyes is possible with the help of TiO_2 and ZnO catalysts (among other catalysts) using combined treatment with cavitation as well as photocatalytic process under the optimized condition. The combined influence of these two phenomena will be determined by the system in question; as a result, optimization is required before operating parameters may be selected for actual operation.

5.2. Effect of external additives

Several external additives can be used to increase the degradation effectiveness in hybrid systems. In this paragraph only final homogeneous systems were discussed (i.e., were additives are soluble in aqueous phase). The various external oxidants includes (hydrogen peroxide, persulfates, carbon tetrachloride (now prohibited, hence it is not used further)), air, ozone, etc. Table 4 summarized the various external additives used for degradation of Rh dyes using AOP based treatments. On the basis of presented data, it is clear that the external additives play an important role in enhancing the rate of degradation as compared to catalysts.

In the case of hydrogen peroxide, the oxidation potential of hydrogen peroxide is quite high despite the fact that it is a weak acid. Higher degradation occurs when hydrogen peroxide is subjected to cavitating conditions because it is converted to hydroxyl radicals (2.8 eV) [158]. In addition, the dissociation of hydrogen peroxide molecules under cavitation conditions produces additional hydroxyl radicals. Increased degradation of Rh B by addition of hydrogen peroxide has been reported by Wang et al. (2009) [159] using a swirling jet hydrodynamic cavitation reactor. It was reported that maximum degradation of 99.1% was obtained at molar ratio of oxidant/pollutant (rox) as 210:1. It should be noted that reported excess is out of reasonable dose, making this process non-economic. Mishra and Gogate (2010) [109] also confirmed an increase of Rh B degradation from 59.3% to 99.9% with addition of oxidant from (expressed as molar ratio of oxidant/pollutant (rox)) 14:1 to 275:1, with a 55% maximum TOC reduction. In a 2013 study, Banerjee et al. (2013) [121] examined the impact of hydrogen peroxide additions on the (170W, 50 kHz)-induced degradation of Rh 6G using ultrasonic irradiation. It was reported, that the rate of decolorization of Rh 6G enhanced up to 77.8% at rox of 1000:1, while 20% rate of decolorization was reported with sole mechanical stirring. Hinge et al. (2016) [107] reported the combined degradation of Rh B and Rh 6 G of 30%–61% for Rh B and 34%–65% for Rh 6G using ultrasonic irradiation, 20%–45% for Rh B and 27%–52% for Rh 6G using ultraviolet irradiation at ratio of 139:1 to 275:1, respectively. Higher dose of H_2O_2 caused decrease of degradation due to self-scavenging of radical species by excess of oxidant molecules. A significant enhancement in degradation to 72% for Rh B and 75% for Rh 6G was reported for combined treatment of US and UV irradiation as predicted. However, still such results should be named as unsatisfactory.

However, as H_2O_2 concentrations increased beyond an optimum limit, the extent of degradation decreased as hydrogen peroxide acts as a scavenger at higher concentrations.

Inorganic ions are often found in industrial wastewater, and therefore it is advisable to establish the effect of these ions on the photocatalytic degradation of dye. Considering these Bhaskar et al. (2013) [103] analyzed the effects of 1.5–4.5 g/L of $FeSO_4$ and $CuSO_4$ for sulfate ions and Na_2CO_3 for carbonate ions using TiO_2/solar irradiations. It was reported that degradation of Rh 6G decreased while concentration of salts increased. At lowest concentration of dissolved salts (1.5 g/L) a 26–32% degradation was obtained (comparing to 9.2% in deionized water) depending on used salt. The maximum degradation of Rh 6G of 96.5% was obtained using optimal TiO_2 (3.0 g/L) + $CuSO_4$ (1.5 g/L). Use of inorganic ions split into cations (Fe^{2+}, Cu^{2+}, Na^{2+}) and sulfate ions (SO_4^{2-}) using solar energy gives additional oxidation mechanisms. Under solar irradiation, sulfate ions can be converted to sulfate radicals and hydroxyl radicals ($OH^{\bullet}$), which provide enhanced degradation of Rh 6G [26,27]. At higher concentrations, anions generally have a scavenging effect, thereby reducing the interactions of the pollutant with generated free radicals and thereby reducing the extent of degradation [28,29].

Mishra and Gogate (2010) [109] studied the effect of carbon tetrachloride (CCl_4) on the degradation of Rh B using hydrodynamic cavitation (venturi). It was reported that around 82% degradation and 34% TOC reduction were obtained using CCl_4, while 59.3% degradation and 30% TOC reduction were obtained in the absence of CCl_4. The increase in the rate of Rhodamine B degradation can be explained by the fact that carbon tetrachloride, a volatile chemical, enters the cavitation bubbles produced cavitation and undergoes a conversion to radical species during the bubbles collapse. This phenomenon yields chlorine-containing radicals (such as *Cl or *CCl_3). Additionally, hydroxyl radicals formed by the sonolysis of water molecules opens a sequence of chain reactions that result in the production of other oxidizing species that can react with target pollutants. This significantly accelerates the Rh B degradation. In other study, usefulness of CCl_4 was confirmed also towards methyl orange degradation under acoustic cavitation conditions. A 160 times increased degradation was reported, resulting in 0.0635 min^{-1} degradation rate in 60 min min [160]. A one of important drawback of this process was relatively high concentration of CCl_4 (1000 ppms) which makes this process not environmentally feasible.

Bokhale et al. (2014) [148] conducted a study in order to better understand the precise role of hydroxyl radicals in the oxidation of Rh 6G in the presence of n-butanol and the probable scavenging activity of methanol. For ultrasonic irradiation experiments, both

n-butanol and methanol were loaded in the 1.5–4.5 ml/L range. In the case of methanol, it was reported that with an increase in the concentration of methanol from 1.5 mL/L to 4.5 mL/L, the extent of degradation also increased from 18.4% to 23.7%. However, in the case of n-butanol, it was reported that the extent of degradation of Rh 6G decreased from 26.0% to 11.9%, which indicates the role of scavenging effect in terms of n-butanol. Higher n-butanol concentrations have adverse impacts. It follows from competitive behaviour in respect to reaction with hydroxyl radicals. The outcome demonstrates that the hydroxyl radical is crucial to the sonolytic breakdown of Rh 6G and that a significant scavenging action has adverse implications. It's also crucial to note that because n-butanol is less volatile than methanol, its greater presence in the bulk results in a stronger scavenging effect on hydroxyl radicals. Overall, hydroxyl radicals are consumed by undesirable reactions of OH* with alcohols, which reduce dye degradation. The activity of alcohols in changing the concentration of the bubbles can also be used to explain an increase in the extent of degradation at lower concentrations of alcohol. According to Riesz et al. (1992) [161], OH radicals can be created either within the bubble itself or at the interface between the bubble and the water in stable cavitation bubbles. There is a possibility that the properties of cavitation bubbles and the formation of radicals during sonication are strongly related to one another. The prolonged expansion duration of bubbles at 50 kHz improves the chance of OH and H radical recombination [161]. This suggests that at lower ultrasonic frequencies, it will be more challenging to transfer OH radicals to the bubble-solution interface. Alcohol can increase the number of active bubbles by adsorbing on the bubble surface during low frequency sonication, which prevents bubble coalescence [162]. The extent of cavitational intensity increases as a result of the increased number of active bubbles, resulting in an overall increase in the level of degradation. Additionally, it is anticipated that methanol will contribute more to increasing the number of active bubbles because it has a greater impact on the stability of cavitation bubbles than n-butanol, leading to higher degradation effectiveness.

In a 2013 study, Banerjee et al. (2013) [121] examined the addition of air during the ultrasonic irradiation (170W, 50 kHz)-induced degradation of Rh 6G. Air-assisted acoustic cavitation increased the rate of decolorization by up to 22.8%. The decolorization of Rh 6 G with ultrasonic irradiation alone was also tested, and it was found that only 9% of Rh 6G was degraded. Hence, it clearly indicates that the introduction of air helps to enhance the degradation by providing additional nuclei to generate cavities, however in overall this process in not effective for Rh 6G degradation. In other study AC was combined with ozone and UV light for degradation of Rh B [163]. Ultrasonic baths with frequencies of 20 kHz, 45 kHz, and 80 kHz. It was reported that the decolorization rate decreased from 97.67% to 72.8% with an increase in initial dye concentration from 50 ppm to 200 ppm. It follows from different mole ratio of oxidant to pollutant (rox) which should be used as optimization parameter, but the authors focused only on one parameter at the time, which limited the applicability of their conclusion. Surprisingly, it was found that the degradation effectiveness was not significantly affected by the solution pH from 2 to 10 and maximum degradation of Rh B was 85.64%, reported at pH 2. Generally, it would be expected to find much higher effectiveness for basic pH which is generally preferred for ozone based AOPs [57,60,164]. Importantly, it was found that the degradation increased along with increase of ultrasounds frequency from 89.02% to 95.24% for 20 kHz and 80 kHz in 10 min, respectively. The best process based on AC-O_3-UV gave 98% degradation in 10 min treatment depending on UV lamp power (8–32W) after 10 min, respectively. It is worth to highlight relatively low power (8W) of UV that revealed to be enough to effectively assist the process. In same time COD removal was almost 40%. On the other hand, almost quantitative degradation obtained in 10 min makes this process reasonable for application in real case scenario.

Huang et al. (2022) [165] investigated the degradation of Rh B assisted by hypocrellins (HYPs) (Ascomycota fungi) using a photocatalytic AOP. It was reported that maximum degradation of Rh B of 82.4% was obtained at alkaline pH using the combined effect of hypocrellins (0.18 mM) and H_2O_2 (0.33% w/w) within 60 min. The degradation of 20.3% and 54.9% was obtained for sole use of H_2O_2 or hypocrellins respectively. It was explained that the HYPs have high photocatalytic activating in the generation of reactive oxygen species (ROS). HYPs showed excellent photochemical properties such as oxygen generated from HYPs via photocatalytic reactions could be captured by hydrogen peroxide, resulting in a promotion of hydroxyl radicals' generation which are considered to be primary ROS agent that targets the organic pollutants and responds to degradation.

When persulfates are activated by heat, light, chemicals, electrochemically, or by cavitation, sulfate radicals as well as hydroxyl radicals are formed. Due to cavitation, additional formation of numerous oxidizing radicals, such as $SO_4^{\bullet-}$, $SO_5^{\bullet-}$, and $HO^{\bullet}$, are responsible for significant degradation based on the possible synergistic effect of cavitation or UV combined with a sulfate system. Zawadzki et al. (2021) [166] investigated the effect of persulfate (PS) in combination with UV and ozone to degrade Rh B. It was reported that maximum degradation of Rh B was 70% in presence of PS while only 17% was reported for sole use of UV irradiation. In another study of same author [167], it was reported that maximum of 49% and 67% of Rh B was degraded using US and UV irradiation in presence of PS (20 mM) in 60 min, while without of oxidant only 29% reduction was observed. The combined operation of US (40 kHz) and UV under optimal PS dose, enhanced the degradation to 85%. Increase of the reaction time to 180 min enhanced the degradation to 95%.

The degradation of Rh 6G using a combined study of US and UV irradiation was also investigated by Banerjee et al. [121]. It was reported that the use of combined treatment of US and UV irradiation was more significant in the presence of hydrogen peroxide. The maximum degradation of 1.5% using UV, 8.7% using US and 20.2% combined operation of US and UV was reported, while in combination with 1 g/L of H_2O_2, the degradation of 70.8% was obtained. In another article a significant improvement of Rh B degradation in the presence of nano-sized ZnO particles under ultrasonic and solar irradiation was reported [154]. A combined process allowed to obtain 100% degradation in just 10 min of treatment time. Beside high effectiveness, the combined treatment process revealed to ensure effective cleaning of photocatalysts surfaces, avoiding accumulation of contaminants or reaction intermediates which provide easy re-use of catalyst.

The comparison of acoustic and hydrodynamic cavitation was also studied by Ye et al. [70] for degradation of Rh B. An ultrasonic horn with a frequency of 20 kHz and a power of 1200 W was compared with a HC system based on a circular venturi with a 2 mm diameter throat section. It was reported that the maximum degradation of Rh B was obtained using ultrasonic cavitation rather than

hydrodynamic cavitation based on the individual optimum conditions. It was also reported that the maximum degradation was comparable for both systems (42% for AC vs 39% for HC in 120 min of treatment).

Gu et al. (2020) [168] used a unique technique of laser cavitation (LC) for treating Rh B dye contaminants. A LC system consisting of laser light of 1064 nm wavelength, 2Hz frequency, and 8 ns pulse width was created to conduct a single cavitation bubble. It was reported, that at 150 mJ (6 mL of volume) of introduced energy, the Rh B (Initial concentration of 20 mg/L) was degraded almost quantitatively (98.4%) after 180 min of treatment time. Rh B was degraded by LC due to thermal decomposition of molecule and reaction with hydroxyl followed by N-de-ethylation, and chromophore group cleavage. Similar mechanism was proposed in the literature also to other types of organic pollutants [95,169–171].

6. Degradation mechanism

The degradation mechanism of Rh dyes has been discussed based on cavitation and photocatalysis processes and is depicted in Fig. 4.

When cavitation or UV light conditions (such as high energy densities) are sufficient, Rh dyes are degraded via an oxidation mechanism that commences with an attack by free radicals on the dye molecule, followed by a reaction with intermediates. During the cavitation phenomenon, Rh dyes undergo degradation mostly by N-de-ethylation process. The Rh dyes were found to be exceptionally stable under irradiation even when there were no catalysts or external oxidants or additives present. Contrarily, when Rh dyes were exposed to ultraviolet light in the presence of any catalysts. The majority of the N-de-ethylation processes were caused by the formation of a nitrogen-centered radical during the degradation of the Rh dyes' chromophore structure. The central carbon of Rh dye may be attacked by photo generated active species like OH* and hole, which will degrade the dye and further degrade Rh dyes via the N-de-ethylation process.

To measure the major by-products of the dye molecule degradation, LC-MS is mostly preferred. However, to obtain more detailed information about the low-molecular (volatile) intermediate products, GC-MS was used. The major intermediate products name and structure of Rh B and Rh 6G have been listed in Table 5. Similar intermediate products formation after degradation of Rh dyes using either cavitation or photocatalysis techniques were also reported [9,69,172,173]. The N-de ethylation process, esterification, carboxylation and dealkylation reactions were reported by various authors during the degradation of Rh dyes. For example, GC/MS results [155] provided strong support for the microwave-enhanced photocatalytic (UV-based) cleavage of Rh B's conjugated xanthene and its N-de-ethylated intermediates [165]. Rh B was N-de-ethylated, and its conjugated structure was further degraded in this system. Following the degradation of Rh B's conjugated structure, two additional steps of degradation were based on ring-opening reaction, resulting in the production of certain carboxylic acids molecules that eventually mineralized into water and carbon dioxide.

The N-de ethylation processes during degradation causes formation of nitrogen radical [47,49,50]. During these processes, the main intermediates had mass to charge ratio (m/z) values from 359 to 443 followed by another possible way of carboxylation process

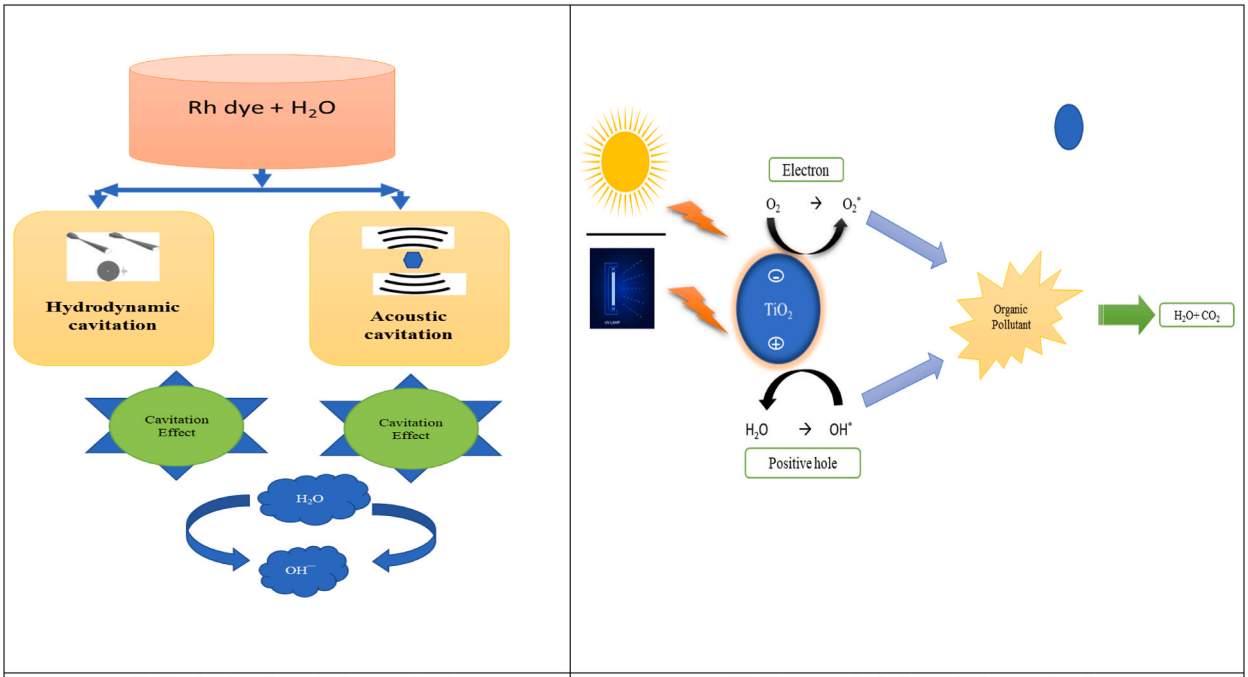

Fig. 4. Degradation mechanism of Rh dyes using cavitation and photocatalysis.

Table 5
Major formed intermediate products name and structure of Rh B and Rh 6G after degradation [11,84,170,171].

m/z value	Name of intermediates	Structure of intermediates
Molecular peak (443)	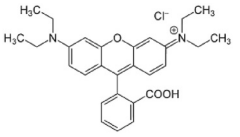	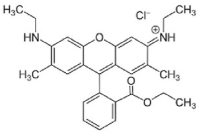
	Rhodamine B	Rhodamine 6G
(415)	(Z)-N-(6-amino-9-(2-(ethoxycarbonyl) phenyl)-2,7-dimethyl-3H-xanthen-3-ylidene)-ethanaminium	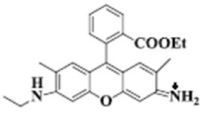
(401)	(Z)-N-(6-amino-9-(2-(ethoxycarbonyl) phenyl)- 2-methyl-3H-xanthen-3-ylidene) ethanaminium	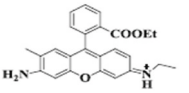
(387)	6-Amino-9-(2-(ethoxycarbonyl)phenyl)- 2,7-dimethyl-3H-xanthen-3-iminium	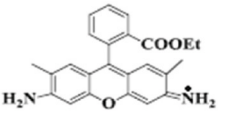
(386)	(E)-N-(9-(2-(ethoxycarbonyl) phenyl)- 7-methyl-3H-xanthen-3-ylidene)- ethanaminium	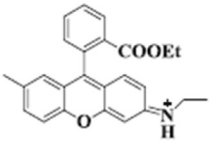
(373)	Ethyl 2-(6-amino-2,7-dimethyl-3H-xanthen-9-yl) benzoate	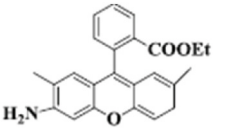
(372)	9-(2-(ethoxycarbonyl) phenyl)- 2,7-dimethyl-3Hxanthen-3-iminium	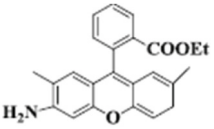
(359)	Ethyl 2-(6-amino-2-methyl-3H-xanthen-9-yl) benzoate	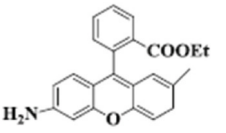
(358)	Ethyl 2-(2,7-dimethyl-3H-xanthen-9-yl) benzoate	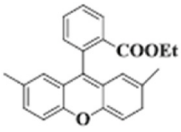
(300)	1,7-dimethyl1-9-phenyl-3H-xanthen-3-iminium	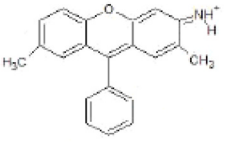
(344)	Ethyl 2-(7-methyl-3H-xanthen-9-yl) benzoate	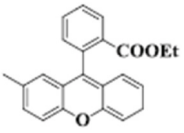
(312)	(Z)-6-(carboxyamino)-3-(ethyliminio)-2,7-dimethyl-3H-xanthen-9-ylium	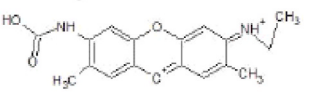

(*continued on next page*)

Table 5 (*continued*)

m/z value	Name of intermediates	Structure of intermediates
(298)	(Z)-6-(carboxyamino)-3-dimethyl-3-(methyliminio)-3H-xanthen-9-ylium	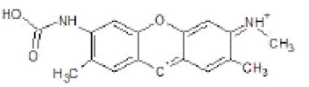
(286)	6-amino-1,7-dimethyl-9-phenyl-3H-xanthen-2-ylium	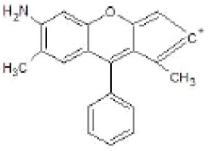
(284)	6-(carboxyamino)-3-iminio-2,7-dimethyl-3H-xanthen-9-ylium	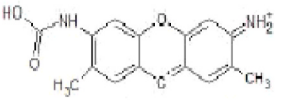
(272)	1,7-dimethyl1-9-phenyl-3H-xanthen	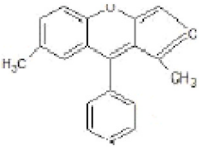
(258)	6-Amino-9-phenylcyclopenta [b] chromenylium	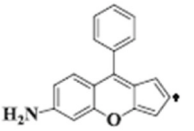
(155)	2-cyno-2propanoic acid	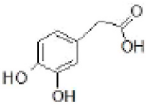
(146)	Adipic acid	
(132)	2-Hydroxypentanedioic acid	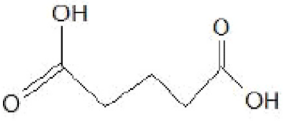
(122)	Benzoic acid	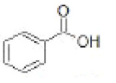
(232)	8-Phenyl-3H-dicyclopenta [b, e] pyran-2,6-diylium	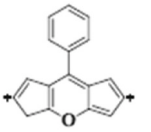
(90)	Oxalic acid	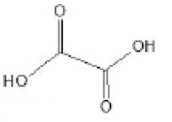

where the intermediates of *m/z* value of 282 to 254 were appeared. After this, the dealkylation process was taken place where these formed intermediates are further oxidized into benzoic acid, phthalic acid, adipic acid, glutaric acid (*m/z* values from 90 to 122) etc. and then further mineralized into carbon dioxide, water, nitrous oxide and ammonia. Intermediate chemicals generated during the degradation of Rh B dye in the presence of conventional irradiation sources are consistent with those described in the published literature [174].

Overall, the reported data suggest that radicals generated during cavitation or other AOPs react with the Rh dye or another organic chemical to produce a wide variety of intermediates. According to reported data it can be stated that Rh dyes can undergo a complete mineralization, with no hazardous by-products being formed.

Table 6
Evaluating acute and chronic toxicities of CBZ and its DPs (in the units of mg/L[a]) towards Fish, Daphnia, and Green Algae.

Compound	Fish (LC_{50})	Daphnia (LC_{50})	Green Algae (EC_{50})	Fish (ChV)	Daphnia (ChV)	Green Algae (ChV)
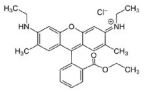 $m/z = 443$	0.037	0.031	0.128	0.006	0.010	0.084
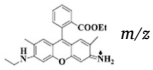 $m/z = 415$	0.143	0.115	0.359	0.021	0.029	0.204
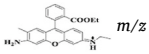 $m/z = 401$	0.363	0.535	0.224	0.006	0.018	0.141
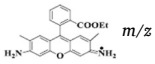 $m/z = 387$	0.703	0.385	0.566	0.010	0.151	0.378
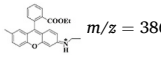 $m/z = 386$	0.127	0.102	0.323	0.019	0.026	0.184
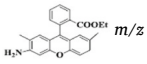 $m/z = 373$	0.637	0.310	0.463	0.008	0.125	0.318
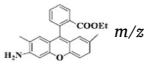 $m/z = 372$	0.164	0.130	0.390	0.024	0.032	0.216
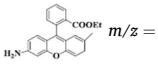 $m/z = 359$	0.899	0.883	0.190	0.015	0.303	0.698
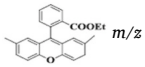 $m/z = 358$	0.036	0.030	0.120	0.006	0.009	0.077
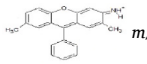 $m/z = 300$	0.260	0.200	0.529	0.036	0.046	0.274
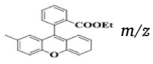 $m/z = 344$	0.107	0.086	0.275	0.016	0.022	0.158
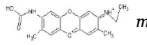 $m/z = 312$	0.743	0.986	0.808	0.022	0.066	0.390
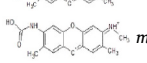 $m/z = 298$	0.990	1.267	1.309	0.035	0.108	0.575
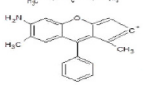 $m/z = 286$	0.560	0.348	0.501	0.008	0.132	0.326
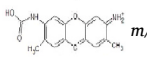 $m/z = 284$	2.04	14.21	14.34	0.065	3.14	5.46
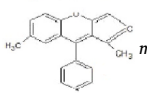 $m/z = 272$	0.147	0.116	0.334	0.021	0.028	0.181
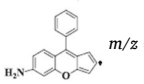 $m/z = 258$	1.086	2.750	3.221	0.025	0.764	1.528
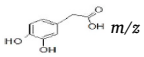 $m/z = 155$	736.394	10608.0	116.10	511.771	4353.366	12.390
 $m/z = 146$	46871.04	22596.1	8557.15	3777.32	1397.58	1556.61
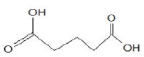 $m/z = 132$	170000	53899.4	16921.4	8936.9	2938.4	2782.4
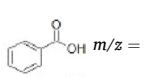 $m/z = 122$	1300.7	730.0	518.3	125.4	68.9	132.2
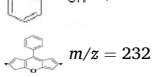 $m/z = 232$	0.105	0.084	0.249	0.015	0.021	0.137
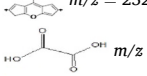 $m/z = 90$	168000	67473.3	12070.3	10917.6	2519.06	1460.6

[a] Estimating acute toxicities in line of European Union criteria (defined in Annex VI of the Directive 67/548/EEC), i.e., $LC_{50} > 100$ or $EC_{50} > 100$ is Not harmful, $10 < LC_{50} < 100$ or $10 < EC_{50} < 100$ is Harmful, $1 < LC_{50} < 10$ or $1 < EC_{50} < 10$ is Toxic, and $LC_{50} < 1$ or $EC_{50} < 1$ is Very toxic and

chronic toxicities were evaluated as per Chinese hazardous compounds evaluation standards (HJ/T154–2004), i.e., ChV>10 is Not harmful, 1< ChV <10 is Harmful, 0.1< ChV <1 is Toxic, and ChV<0.1 is Very toxic.

It is crucial to assess the toxicity of the Rh dye's family by-products produced during their degradation. In order to assess the acute toxicity of each by-product that is produced after the degradation in relation to standard organisms, an Ecological Structure Activity Relationships (ECOSAR) study for the Rh dye family was conducted in this evaluation in accordance with European Union guidelines. The details of the assessed acute and chronic toxicities of CBS and its DP value in mg/L for fish, daphnia, and green algae are provided in Table 6. According to Table 6, the majority of the by-products created after Rh dye degradation are highly hazardous. It was particularly observed for by-products having molecular mass in the range of 232–443. The intermediates having lower molecular mass revealed to have much lower toxicity. It follows from their less complex structure and lower number of peripherial functional groups making them more inert towards test organisms. Furthermore, it was found that green algae were the most sensitive indicator for analyzed by-products. Most frequently, the less severe acute and chronic toxicity was observed for lowers molecular mass by-products (90–155 g/mol range). It confirms the need of effective mineralization of primary pollutants to provide really treated effluent.

To the best of our knowledge, this work is the first attempt to comprehensively analyse toxicological effects of the Rh dye family and their degradation by-products using standard organisms. This should serve as motivation for future research on how organisms behave when exposed to Rh dyes. The results of the toxicological assessment serve as a warning about the toxicity of the Rh dye family and the ineffectiveness of the suggested treatment for reducing these effects.

7. Energy efficiency and cost analysis for hydrodynamic cavitation reactors

After understanding the dependency of optimized parameters and intensified techniques for the efficient degradation of Rh dyes, it is important to evaluate the technical and economic feasibility of any process at an industrial scale of operation. Cost and energy efficiency are among the decisive factors that pave the way for up-gradation of any process. The comprehensive details of important data related to cost and degradation have been reported in Table 7. The pump, ultrasonic transducers, and UV lamp are the major components, whereas the cavitating device, piping, electrical connections, and reactor body are the minor components in hydrodynamic cavitation, ultrasonic irradiation, and ultraviolet irradiation, respectively. The major components of all three treatment techniques play a decisive role in the treatment cost. In addition to that, the effect of operating parameters such as treatment time, volume of reaction, temperature, stirring speed, and volume of reaction plays an important role in deciding the economic feasibility of the process. For instance, the inlet pressure, ultrasonic frequency, and power of the ultraviolet lamp of respective treatment techniques and their treatment time directly affect the cost of the treatment. Thus, it can be said that the cost of the treatment is more sensitive to the treatment time rather than the other operating process parameters based on the reactor (inlet pressure, ultrasonic frequency, etc.). Choice of component also plays an important role in the overall cost and efficiency of process. For instance, in one of the recent studies by Roy and Moholkar [119], while using a positive displacement pump of 1.1 kW power rating, it was reported that the optimum inlet pressure was 3 when a slit venturi was used, whereas the optimum inlet pressure was 5 bar when a circular venturi and orifice plate were used. Hence, it can be clearly established here that the slit venturi gives significant degradation at lower operating conditions as compared to the required operating conditions of the circular venturi and orifice plate. Even though the fabrication of the venturi is more complicated and costlier than the orifice plate, the slit venturi is still preferred for the degradation purpose due to its lower pressure drop. Consequently, more cavities are generated and collapsed, which reduces the treatment time and, hence, the operating costs will be lower with the use of slit venturi. Das and Gogate reported that the treatment cost required for 29% degradation of Rh dyes using slit venturi [69] was US$13.7/m^3, which is quite lower than the circular venturi [68] (US$ 32.2/m^3 for 23% degradation) and orifice plate [68] (US$ 36/m^3 for 20% degradation). This energy efficiency can be calculated in terms of cavitational yield, which can be defined as the observed extent of degradation of the pollutant per unit of energy supplied to the system [113]. In their investigation, Gu et al. [168] reported that the cavitational yield was found to be higher in the case of laser cavitation as compared to hydrodynamic cavitation. It was also reported that when the degradation of Rh B was in the range of 70.8%–98.4%, then the cavitational yield was in the range of 3.64×10^{-5} to 7.87×10^{-5} which is quite larger than the hydrodynamic cavitation (cavitational yield of 1.50×10^{-6} to 6.59×10^{-5} for 15%–87%) and acoustic cavitation (cavitational yield of 1.56×10^{-6} to 2.97×10^{-6} for 45%–88%). This increased cavitational yield was reported due to the higher Rh B degradation and lower power dissipation per unit volume. Thus, overall, it can be easily established here that hydrodynamic cavitation is more energy efficient than acoustic cavitation. Furthermore, using additives and catalysts in combination with other AOPs techniques (cavitation or ultraviolet irradiation) can reduce operating costs by producing a synergistic effect that increases oxidant formation while decreasing treatment time [175,176].

8. Design of reactors and recommendations for future work

When employing a cavitation reactor to improve Rh dye degradation, it's critical to increase the cavitational yield, which measures how much degradation occurs per unit of introduced energy. The collapse intensity, which in turn depends on the cavity life, size, and collapse time, determines the cavitational yield. The type of cavitating device, inlet pressure, and other parameters all influence these variables. Following a thorough review of the current literature, we've compiled a list of design and scaling-up strategy suggestions.

One of the most important factors in determining the maximum rhodamine degradation is the type of cavitating device used (orifice or venturi). Flow geometry, the size of the constriction, and the size of the pipe all influence the choice of cavitating devices like orifice and venturi. The cavitation number can be decreased, which raises the cavitational intensity, with the right flow shape and pipe size. It should be noted that using an orifice rather than a venturi may be more advantageous since it allows for the achievement of maximal

Table 7
Detailed data of degradation of Rh dyes using various methods.

Method	Device	Pressure (Bar)	Initial Concen. (ppm)	Final concen (ppm)	Volume (L)	Time (min)	% Degradation	Power density (J/L)	Cavitational Yield (mg/J)	Ref
HC/Rh B	Venturi	6	5	1.25	4	120	25	1.98×10^{6}	6.31×10^{-7}	[68]
HC/Rh B	Orifice	6	5	1.25	4	120	20	1.98×10^{6}	5.05×10^{-7}	[68]
HC/Rh B	Orifice	4	3	0.441	50	169	14.7	6.08×10^{5}	7.24×10^{-7}	[177]
HC/Rh B	Swirling	4	3	0.747	50	169	24.9	1.62×10^{5}	4.60×10^{-6}	[177]
HC/Rh 6G	Slit venturi	7	10	3.206	6	120	32.06	2.64×10^{6}	1.21×10^{-6}	[69]
HC/Rh 6G	Slit venturi	7	10	2.965	6	120	29.65	2.64×10^{6}	1.12×10^{-6}	[69]
HC/Rh B	Circular venturi	4	10	3.87	4	120	38.7	5.40×10^{6}	7.16×10^{-7}	[70]
US/Rh B	US	–	10	3.66	0.25	90	36.6	1.72×10^{7}	2.11×10^{-7}	[70]
US/Rh 6G	170W, 50 kHz	–	10	2.9	2	180	29	9.18×10^{5}	3.15×10^{-6}	[107]
Laser cavitation	2Hz	–	20	14.16	6	180	70.8	1.80×10^{5}	7.87×10^{-5}	[168]
Laser cavitation	2Hz	–	20	19.68	6	180	98.4	5.40×10^{5}	3.64×10^{-5}	Gu et al. [168]

intensity, which improves treatment effectiveness — especially for complicated effluents — by allowing for more intensity. It may be claimed that when comparing the circular and slit venturi, the slit venturi is preferable because it results in increased cavitational activity. It is vital to note that the best cavitation number is often between 0.15 and 0.2, which is based on the correct selection of the geometries and finely the defined cavitation number is obtained by proper linear velocity of the fluid through the constriction regulated by volumetric flowrate or diameter of the constriction. Various orifice plate designs that might be used in hydrodynamic cavitation are depicted on Fig. 5.

Studying the cavitational intensity when two half holes with lower diameters and the same or different sizes in the orifice plate are combined is fascinating. In case IV (Fig. 5), where plates have various layouts of smaller and larger diameter holes, better results are obtained. Higher turbulence is produced by holes with a smaller diameter, while higher cavitational intensities are produced by holes with a bigger shear layer area.

There have been a few fascinating designs of hydrodynamic cavitational-based reactors documented by various researchers. Xu et al.(2010) [178], reported air-bubble cavitation using small glass balls. In this technique, the authors created a 1 L lab-scale equipment filled with 3.0 mm–3.5 mm glass marbles. The reactor is a 10-cm-diameter, 30-cm-tall cylindrical tank. The batch reactor was pumped from the bottom with air. During the process, original air bubbles were split up by little glass balls, resulting in many small bubbles. In order to lower surface tension and energy, two or more little air bubbles quickly unite to produce a larger one. When the inner wall tension between two bubbles reaches a maximum limit, it bursts and collapses rapidly, as in cavitation. Using this innovative cavitation approach, methyl orange dye was degraded by 37.82% at optimized reaction conditions. Other dyes were degraded by 60.73%, 64.52%, 71.75%, and 76% using the same procedure and operating conditions: Rhodamine B, Congo Red, Azo Fuchsin, and Acid Red B. Mahale et al. (2016) [179] also reported that the maximum degradation of 73.1% with 36.6% COD removal of patent blue V under optimized conditions (pH 7.2, initial concentration of 20 ppm, air flow rate of 4.5 mL/min, pH of 6). Further improvement was reported with addition of catalysts (83.4%, 60.5% COD removal) for 0.6 g/L of TiO_2 and additives (97.0%, 68.1% COD removal) for 0.3 g/L of Fenton reagent [180]. Badve et al. (2014) [181] revealed another significant novel high-speed homogenizer design that includes a stator and rotor through which cavitation was produced. An electric motor, a stator, and a rotor make up the reactor. A stator and a rotor are separated by a small annular gap. Both the rotor and the stator have grooves, each of which has a particular geometry and serves as a barrier to maintain high pressure outside the cavitation zone [182]. According to reports, it was possible to reduce COD by 49%, while the addition of 5 g/L of hydrogen peroxide gave 89% COD reduction. In addition, Patil et al. (2021) [183] reported employing a combined air and vortex diode to achieve a vortex-based cavitating device in hydrodynamic cavitation with a maximal TOC reduction of 74% for octanol (200 ppm). There are no studies reported yet for the degradation of rhodamine dye using above mentioned cavitating reactors hence, it is recommended to utilize the above reactors for the effective degradation of rhodamine dyes.

The combination of solar light or UV with hydrodynamic cavitation should give good synergism for Rh dyes removal, as such systems proved to be effective for other types of organic pollutants [31]. Up till now, there is no published works on this aspect. In order to combine photocatalysts with solar energy, it is advised to alter the hydrodynamic cavitation reactor's feed tank. The feed tank can be slanted or adjusted to allow direct solar light to enter, or solar plates can be placed on top of the feed tank to induce hydrodynamic cavitation. Another inexpensive way to improve the process is the solar pumps.

There are two ways to operate an ultrasonic reactor on a large scale: combining numerous small ultrasonic reactors sequentially or building a single large reactor [96]. It may be concluded that tubular or hexagonal ultrasonic reactors are recommended for large-scale and continuous operation due to many transducers (placed on the reactor walls) and variable frequency operation so that total costs can be minimized while achieving the required intensities [96]. A consistent and essential cavitational activity in the reactor can be achieved using theoretical models for reactor design optimization.

While designing a photocatalytic reactor at a large-scale operation, there are many factors that need to be considered such as the selection of light source, reactor shape, intensity distribution, and also the kind and loading of the photocatalyst etc, and hence, the designing of a photoreactor is a lengthy process. The investigators reported a variety of photocatalytic reactor designs, including parabolic troughs, flat plates, and falling film photoreactors [63,184]. Bhatkhande et al. (2003) [185] explored scale-up aspects for

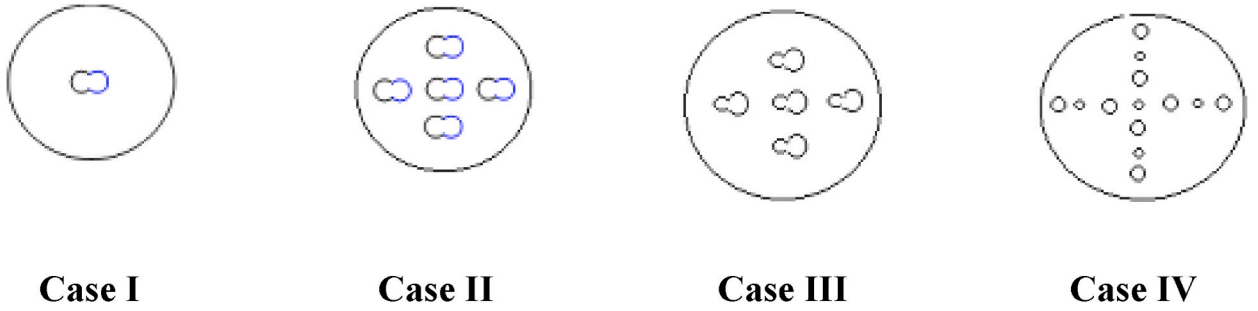

Fig. 5. Various possible designs for orifice plate.
Case I: Two half-holes that are connected and have the same size smaller diameters; Case II: Two half-holes with smaller diameters that are joined together, with one little and the other large; Case-III: A combination of more than two half-holes with smaller diameters and the same size and diverse arrangements; Case IV: A combination of more than two half-holes with smaller diameters and the same size and diverse arrangements.

nitrobenzene degradation, concluding that the rate of nitrobenzene degradation decreased from 15.5 to 1.5 mg/(L.min) as reactor volume increased from 0.25 to 2L. The main issue relates to limited penetration intensity of the light into the solution for larger-volume reactors. Though the reactors can be obtained effective degradation of dyes in the presence of various photocatalysts, the costs associated with their manufacturing are crucial [186]. Still, the scale-up of photocatalytic reactors necessitates a more in-depth investigation.

With an objective of developing efficient technology for large-scale operation for the effective removal of Rh dyes from wastewater, the following areas of concern needs to be addressed:

a) It is preferable to treat wastewater containing Rh dyes at a lower concentration rather than with a higher concentration. Intended dilution of effluents prior to treatment may be impractical owing to the enormous volumes involved. As a result, efforts should be made to develop a technology that can disintegrate high-concentration Rh dyes in wastewater.
b) In photocatalytic treatment, it is recommended to utilize solar energy instead of UV light to reduce treatment costs. It's also intriguing to see how solar energy is used in the feed tank of the hydrodynamic cavitation reactor with the appropriate modification. The feed tank may be of the tilting or sliding type to allow for the direct penetration of solar light; alternatively, solar plates may be used on the top of the feed tank in order to achieve hydrodynamic cavitation.

9. Conclusions

The current study focused on various aspects of Rh dye degradation using hydrodynamic cavitation, ultrasonic cavitation and photocatalysis. Furthermore, it has been revealed that a number of operating parameters, including pH, temperature, the initial concentration of the pollutant affects the efficiency of degradation. On the basis of reviewed material, some crucial observations can be formed:

1. Significant degradation of Rh dyes can be obtained under hydrodynamic cavitation in the order of slit venturi > circular venturi > multiple-hole orifice plate > single-hole orifice plate (not more than 2 mm diameter of the constriction). In this case effective cavitation condition are obtained at inlet pressure values of 3–5 bars, providing cavitation number between 0.05 and 0,4.
2. In case of acoustic cavitation, frequency of 20–40 kHz at power density in the range of 100–200 W/dm^3) revealed to provide optimum performance.
3. According to available literature, Rh dyes are present in industrial effluents on 1–100 (mg/L) ppm level. Optimal process conditions for effective treatment demand low initial dye concentration of 5–10 ppm, average temperature between 30 and 40°C, average stirring speed (500–700 rpm).
4. Importantly, treatment conditions must be adjusted depending on pollutant treated in respect to pH. In case Rh B pH should be 2–4, while for Rh 6G it should be 9–13. However, for UV assisted processes, the acidic pH favours higher degradation for both dyes.
5. To intensify the degradation process, various catalysts (TiO_2, MnO_2, CuO, ZnO, etc.), external oxidants external oxidants (H_2O_2, air, O_3, persulfate etc.) and additives (NaCl, surfactants etc.) revealed to significanlty increase the effectivenss.
6. Combined techniques such as photocatalysis in conjunction with hydrodynamic cavitation or other cavitating reactors such as vortex-diode, high-speed homogenizer and cavity-bubble induced oxidation also holds great promise for Rh dye degrading efficiency and scalability.
7. Laser cavitation solely gives higher degradation than the other cavitating types. However, more studies should be performed for this technique to fully evaluate its practical value.
8. Photo Fenton-Peracetic Acid (PAA) is one of the options for achieving total degradation of Rh dyes, along with hydrogen peroxide and HC + Ozone. Overall, the efficacy of advanced oxidational processes based cavitational and ultraviolet irradiation reactors can be clearly established for the removal of harmful and toxic Rh dyes in terms of economic feasibility and significant degradation.
9. Photo-Fenton-PAA and Fenton-Peracetic Acid (PAA) process was found to be the most efficient for complete degradation of Rh dyes in a short time (5–10 min).

Declaration of competing interest

The authors declare that they have no known competing financial interests or personal relationships that could have appeared to influence the work reported in this paper.

Data availability

No data was used for the research described in the article.

Appendix A. Supplementary data

Supplementary data to this article can be found online at https://doi.org/10.1016/j.wri.2023.100220.

References

[1] T.E.M. Foundation, A New Textiles Economy: Redesigning Fashion's Future, the Ellen Macarthur Foundation, 2017.
[2] B. Lellis, C.Z. Fávaro-Polonio, J.A. Pamphile, J.C. Polonio, Effects of textile dyes on health and the environment and bioremediation potential of living organisms, Biotechnology Research and Innovation 3 (2019) 275–290, https://doi.org/10.1016/j.biori.2019.09.001.
[3] K. Bailey, A. Basu, S. Sharma, The environmental impacts of fast fashion on water quality: a systematic review, Water (Switzerland) 14 (2022), https://doi.org/10.3390/w14071073.
[4] D.A. Yaseen, M. Scholz, Textile Dye Wastewater Characteristics and Constituents of Synthetic Effluents: a Critical Review, Springer Berlin Heidelberg, 2019, https://doi.org/10.1007/s13762-018-2130-z.
[5] S.M. Ghoreishi, R. Haghighi, Chemical catalytic reaction and biological oxidation for treatment of non-biodegradable textile effluent, Chem. Eng. J. 95 (2003) 163–169, https://doi.org/10.1016/S1385-8947(03)00100-1.
[6] M.N.A. Al-Tameemi, Detection of gain enhancement in laser-induced fluorescence of rhodamine B lasing dye by silicon dioxide nanostructures-coated cavity, Photonic Sensors 8 (2018) 80–87, https://doi.org/10.1007/s13320-017-0462-9.
[7] M.Y.S. Kumawat, D.A.D. Kulkarni, M.-T. Scholar, B. Vidyapeeth, Treatment of textile wastewater containing rhodamine B using advance oxidation processes, International Journal of Scientific Development and Research 2 (2017) 48–59.
[8] F.M. Zehentbauer, C. Moretto, R. Stephen, T. Thevar, J.R. Gilchrist, D. Pokrajac, K.L. Richard, J. Kiefer, Fluorescence spectroscopy of Rhodamine 6G: concentration and solvent effects, Spectrochim. Acta Mol. Biomol. Spectrosc. 121 (2014) 147–151, https://doi.org/10.1016/j.saa.2013.10.062.
[9] T. Rasheed, M. Bilal, H.M.N. Iqbal, H. Hu, X. Zhang, Reaction mechanism and degradation pathway of rhodamine 6G by photocatalytic treatment, Water Air Soil Pollut. 228 (2017), https://doi.org/10.1007/s11270-017-3458-6.
[10] H. Du, Y. Zhang, H. Jiang, H. Wang, Environmental Technology & Innovation Adsorption of rhodamine B on polyvinyl chloride , polystyrene , and polyethylene terephthalate microplastics in aqueous environments, Environ. Technol. Innov. 27 (2022), 102495, https://doi.org/10.1016/j.eti.2022.102495.
[11] K. Kolmakov, V.N. Belov, J. Bierwagen, C. Ringemann, V. Müller, C. Eggeling, S.W. Hell, Red-emitting rhodamine dyes for fluorescence microscopy and nanoscopy, Chem. Eur J. 16 (2010) 158–166, https://doi.org/10.1002/chem.200902309.
[12] S. elbakry, M.E.A. Ali, M. Abouelfadl, N.A. Badway, K.M.M. Salam, Effective removal of organic compounds using a novel cellulose acetate coated by PA/g-CN/Ag nanocomposite membranes, Surface. Interfac. 29 (2022), 101748, https://doi.org/10.1016/j.surfin.2022.101748.
[13] A. Mehrdad, R. Hashemzadeh, Ultrasonic degradation of Rhodamine B in the presence of hydrogen peroxide and some metal oxide, Ultrason. Sonochem. 17 (2010) 168–172, https://doi.org/10.1016/j.ultsonch.2009.07.003.
[14] M.C. Ugwu, A. Oli, C.O. Esimone, R.U. Agu, Organic cation rhodamines for screening organic cation transporters in early stages of drug development, J. Pharmacol. Toxicol. Methods 82 (2016) 9–19, https://doi.org/10.1016/j.vascn.2016.05.014.
[15] N. Tripathi, Cationic and anionic dye adsorption by agricultural solid wastes: a comprehensive review by, IOSR J. Appl. Chem. 5 (2013) 91–108, https://doi.org/10.9790/5736-5391108.
[16] W.S. Kuo, P.H. Ho, Solar photocatalytic decolorization of methylene blue in water, Chemosphere 45 (2001) 77–83, https://doi.org/10.1016/S0045-6535(01)00008-X.
[17] J.H. Sun, S.P. Sun, J.Y. Sun, R.X. Sun, L.P. Qiao, H.Q. Guo, M.H. Fan, Degradation of azo dye Acid black 1 using low concentration iron of Fenton process facilitated by ultrasonic irradiation, Ultrason. Sonochem. 14 (2007) 761–766, https://doi.org/10.1016/j.ultsonch.2006.12.010.
[18] M.L. Sikosana, K. Sikhwivhilu, R. Moutloali, D.M. Madyira, Municipal wastewater treatment technologies: a review, in: Procedia Manuf, Elsevier B.V., 2019, pp. 1018–1024, https://doi.org/10.1016/j.promfg.2019.06.051.
[19] M.D. Vedenyapina, A.Y. Kurmysheva, A.K. Rakishev, Y.G. Kryazhev, Activated carbon as sorbents for treatment of pharmaceutical wastewater (Review), Solid Fuel Chem. 53 (2019) 382–394, https://doi.org/10.3103/S0361521919070061.
[20] K. Shen, M.A. Gondal, Removal of hazardous Rhodamine dye from water by adsorption onto exhausted coffee ground, J. Saudi Chem. Soc. 21 (2017), https://doi.org/10.1016/j.jscs.2013.11.005. S120–S127.
[21] S.F. Anis, R. Hashaikeh, N. Hilal, Microfiltration membrane processes: a review of research trends over the past decade, J. Water Proc. Eng. 32 (2019), https://doi.org/10.1016/j.jwpe.2019.100941.
[22] M.v. Bagal, P.R. Gogate, Degradation of 2,4-dinitrophenol using a combination of hydrodynamic cavitation, chemical and advanced oxidation processes, Ultrason. Sonochem. 20 (2013) 1226–1235, https://doi.org/10.1016/j.ultsonch.2013.02.004.
[23] L.K. Sanghavi, S.V. Ranga, A study of removal of basic violet 14 dye using prosopis juliflora bark, Bull. Environ. Sci. Res. 7 (2017) 1–6, https://doi.org/10.13140/RG.2.2.15131.31524.
[24] a L. Ahmad, L.S. Tan, S.R.A. Shukor, Dimethoate and atrazine retention from aqueous solution by nanofiltration membranes, J. Hazard Mater. 151 (2008) 71–77, https://doi.org/10.1016/j.jhazmat.2007.05.047.
[25] R. Kidak, N.H. Ince, Ultrasonic destruction of phenol and substituted phenols: a review of current research, Ultrason. Sonochem. 13 (2006) 195–199, https://doi.org/10.1016/j.ultsonch.2005.11.004.
[26] L. Zeng, J.W. McKinley, Degradation of pentachlorophenol in aqueous solution by audible-frequency sonolytic ozonation, J. Hazard Mater. 135 (2006) 218–225, https://doi.org/10.1016/j.jhazmat.2005.11.051.
[27] A.R. Rahmani, R.A. Gilan, G. Asgari, M. Leili, A. Dargahi, Enhanced degradation of Rhodamine B dye by Fenton/peracetic acid and photo-Fenton/peracetic acid processes, Int. J. Chem. React. Eng. (2022) 1–16, https://doi.org/10.1515/ijcre-2022-0008.
[28] M. Kida, S. Ziembowicz, P. Koszelnik, Removal of organochlorine pesticides (OCPs) from aqueous solutions using hydrogen peroxide, ultrasonic waves, and a hybrid process, Sep. Purif. Technol. 192 (2018) 457–464, https://doi.org/10.1016/j.seppur.2017.10.046.
[29] A.J. Barik, P.R. Gogate, Degradation of 4-chloro 2-aminophenol using a novel combined process based on hydrodynamic cavitation, UV photolysis and ozone, Ultrason. Sonochem. 30 (2016) 70–78, https://doi.org/10.1016/j.ultsonch.2015.11.007.
[30] V. Mahendran, P.R. Gogate, Degradation of Acid Scarlet 3R dye using oxidation strategies involving photocatalysis based on Fe doped TiO2 photocatalyst, ultrasound and hydrogen peroxide, Sep. Purif. Technol. 274 (2021), 119011, https://doi.org/10.1016/j.seppur.2021.119011.
[31] K. Fedorov, K. Dinesh, X. Sun, R. Darvishi, C. Soltani, Z. Wang, S. Sonawane, G. Boczkaj, Synergistic effects of hybrid advanced oxidation processes (AOPs) based on hydrodynamic cavitation phenomenon – a review, Chem. Eng. J. 432 (2022), 134191, https://doi.org/10.1016/j.cej.2021.134191.
[32] F. Rüdiger, D. Paustian, M. Deggelmann, N. Julius-alexander, P. Braeutigam, Ultrasonics Sonochemistry Hydrodynamic Cavitation for Micropollutant Degradation in Water – Correlation of Bisphenol A Degradation with Fluid Mechanical Properties, 2022, p. 83, https://doi.org/10.1016/j.ultsonch.2022.105950.
[33] S. Das, A.P. Bhat, P.R. Gogate, Journal of Water Process Engineering Degradation of dyes using hydrodynamic cavitation : process overview and cost estimation, J. Water Proc. Eng. 42 (2021), 102126, https://doi.org/10.1016/j.jwpe.2021.102126.
[34] Y.L. Pang, A.Z. Abdullah, S. Bhatia, Review on sonochemical methods in the presence of catalysts and chemical additives for treatment of organic pollutants in wastewater, Desalination 277 (2011) 1–14, https://doi.org/10.1016/j.desal.2011.04.049.
[35] M. Pera-Titus, V. Garcıa-Molina, M. a Baños, J. Giménez, S. Esplugas, Degradation of chlorophenols by means of advanced oxidation processes: a general review, Appl. Catal., B 47 (2004) 219–256, https://doi.org/10.1016/j.apcatb.2003.09.010.
[36] A.S. González, S.S. Martínez, Study of the sonophotocatalytic degradation of basic blue 9 industrial textile dye over slurry titanium dioxide and influencing factors, Ultrason. Sonochem. 15 (2008) 1038–1042, https://doi.org/10.1016/j.ultsonch.2008.03.008.
[37] P.R. Gogate, A.B. Pandit, A review of imperative technologies for wastewater treatment I: oxidation technologies at ambient conditions, Adv. Environ. Res. 8 (2004) 501–551, https://doi.org/10.1016/S1093-0191(03)00032-7.
[38] P.R. Gogate, Cavitational reactors for process intensification of chemical processing applications: a critical review, Chem. Eng. Process: Process Intensif. 47 (2008) 515–527, https://doi.org/10.1016/j.cep.2007.09.014.

[39] Y.-S. Ma, C.-F. Sung, J.-G. Lin, Degradation of carbofuran in aqueous solution by ultrasound and Fenton processes: effect of system parameters and kinetic study, J. Hazard Mater. 178 (2010) 320–325, https://doi.org/10.1016/j.jhazmat.2010.01.081.

[40] H. Sun, J. Qin, L. Yi, Y. Ruan, J. Wang, D. Fang, A new process for degradation of Auramine O dye and heat generation based on orifice plate hydrodynamic cavitation (HC) Parameter optimization and performance analyses, Process Saf. Environ. Protect. 161 (2022) 669–683, https://doi.org/10.1016/j.psep.2022.03.058.

[41] H.J. Fan, S.T. Huang, W.H. Chung, J.L. Jan, W.Y. Lin, C.C. Chen, Degradation pathways of crystal violet by Fenton and Fenton-like systems: condition optimization and intermediate separation and identification, J. Hazard Mater. 171 (2009) 1032–1044, https://doi.org/10.1016/j.jhazmat.2009.06.117.

[42] A.L. Patil, P.N. Patil, P.R. Gogate, Degradation of imidacloprid containing wastewaters using ultrasound based treatment strategies, Ultrason. Sonochem. 21 (2014) 1778–1786, https://doi.org/10.1016/j.ultsonch.2014.02.029.

[43] P.S. Bapat, P.R. Gogate, A.B. Pandit, Theoretical analysis of sonochemical degradation of phenol and its chloro-derivatives, Ultrason. Sonochem. 15 (2008) 564–570, https://doi.org/10.1016/j.ultsonch.2007.08.002.

[44] R. Chand, N.H. Ince, P.R. Gogate, D.H. Bremner, Phenol degradation using 20, 300 and 520 kHz ultrasonic reactors with hydrogen peroxide, ozone and zero valent metals, Sep. Purif. Technol. 67 (2009) 103–109, https://doi.org/10.1016/j.seppur.2009.03.035.

[45] K.P. Mishra, P.R. Gogate, Ultrasonic degradation of p-nitrophenol in the presence of additives at pilot scale capacity, Ind. Eng. Chem. Res. 51 (2012) 1166–1172, https://doi.org/10.1021/ie2023806.

[46] P.R. Gogate, A.B. Pandit, A review of imperative technologies for wastewater treatment II: hybrid methods, Adv. Environ. Res. 8 (2004) 553–597, https://doi.org/10.1016/S1093-0191(03)00031-5.

[47] P.R. Gogate, Cavitation: an auxiliary technique in wastewater treatment schemes, Adv. Environ. Res. 6 (2002) 335–358, https://doi.org/10.1016/S1093-0191(01)00067-3.

[48] P.R. Gogate, R.K. Tayal, A.B. Pandit, Cavitation : A Technology on the Horizon, 2006, p. 91.

[49] A.S. Mhetre, P.R. Gogate, New design and mapping of sonochemical reactor operating at capacity of 72L, Chem. Eng. J. 258 (2014) 69–76, https://doi.org/10.1016/j.cej.2014.07.075.

[50] Z. Rahmani, M. Kermani, M. Gholami, A.J. Jafari, N.M. Mahmoodi, Effectiveness of photochemical and sonochemical processes in degradation of basic violet 16 (BV16) dye from aqueous solutions, Iran. J. Environ. Health Sci. Eng. 9 (2012) 1–7, https://doi.org/10.1186/1735-2746-9-14.

[51] M. Li, A. Bussonnière, M. Bronson, Z. Xu, Q. Liu, Study of Venturi tube geometry on the hydrodynamic cavitation for the generation of microbubbles, Miner. Eng. 132 (2019) 268–274, https://doi.org/10.1016/j.mineng.2018.11.001.

[52] P.S. Kumar, A.B. Pandit, Modeling hydrodynamic cavitation, Chem. Eng. Technol. 22 (1999) 1017–1027, https://doi.org/10.1002/(SICI)1521-4125(199912)22:12.

[53] P.R. Gogate, Application of cavitational reactors for water disinfection: current status and path forward, J. Environ. Manag. 85 (2007) 801–815, https://doi.org/10.1016/j.jenvman.2007.07.001.

[54] A.V. Mohod, P.R. Gogate, G. Viel, P. Firmino, R. Giudici, Intensification of biodiesel production using hydrodynamic cavitation based on high speed homogenizer, Chem. Eng. J. 316 (2017), https://doi.org/10.1016/j.cej.2017.02.011.

[55] B. Wang, T. Wang, H. Su, Hydrodynamic cavitation (HC) degradation of tetracycline hydrochloride (TC), Sep. Purif. Technol. 282 (2022), 120095, https://doi.org/10.1016/j.seppur.2021.120095.

[56] V.K. Saharan, M.A. Rizwani, A.A. Malani, A.B. Pandit, Effect of geometry of hydrodynamically cavitating device on degradation of orange-G, Ultrason. Sonochem. 20 (2013) 345–353, https://doi.org/10.1016/j.ultsonch.2012.08.011.

[57] K. Fedorov, K. Dinesh, X. Sun, R. Darvishi Cheshmeh Soltani, Z. Wang, S. Sonawane, G. Boczkaj, Synergistic effects of hybrid advanced oxidation processes (AOPs) based on hydrodynamic cavitation phenomenon – a review, Chem. Eng. J. 432 (2022) 24–27, https://doi.org/10.1016/j.cej.2021.134191.

[58] M. Gągol, A. Przyjazny, G. Boczkaj, Wastewater treatment by means of advanced oxidation processes based on cavitation – a review, Chem. Eng. J. 338 (2018) 599–627, https://doi.org/10.1016/j.cej.2018.01.049.

[59] G. Boczkaj, M. Klein, A. Przyjazny, Effective method of treatment of effluents from production of bitumens under basic pH conditions using hydrodynamic cavitation aided by external, Oxidants Ultrasonic Sonoche. 40 (2018) 969–979, https://doi.org/10.1016/j.ultsonch.2017.08.032.

[60] A. Przyjazny, G. Boczkaj, Effective method of treatment of industrial effluents under basic pH conditions using acoustic cavitation processes, Chem. Eng. Process Inenstific. (2018) 103–113, https://doi.org/10.1016/j.cep.2018.04.010.

[61] M.K.N. Yenkie, Photo-oxidative degradation of synthetic organic pollutant p -, nitrophenol,, J. Scientific. Indust. Res. 63 (2004) 518–521.

[62] A.S. Stasinakis, Use of selected advances oxidation processes (AOPs) for wastewater treatment, A mini review, Global NEST J. 10 (2008) 376–385.

[63] L. Matoh, B. Žener, R. Cerc Korošec, U.L. Štangar, Photocatalytic water treatment, in: Nanotechnology in Eco-Efficient Construction: Materials, Processes and Applications, 2018, pp. 675–702, https://doi.org/10.1016/B978-0-08-102641-0.00027-X.

[64] S. Hiremath, C Vidya, M. Antonyraj, M. Chandraprabha, S. Seemashri, B. Shetty, A. Belamkar, R. Nair, Photocatalytic degradation study of Rhodamine-B by green synthesized nano TiO_2, Asian J. Chem. 29 (2017) 221–225.

[65] M.V. Bagal, P.R. Gogate, Photocatalytic and Sonophotocatalytic degradation of alachlor using different photocatalyst, Adv. Environ. Res. 2 (2013) 261–277, https://doi.org/10.12989/aer.2013.2.4.261.

[66] M.V. Bagal, P.R. Gogate, Wastewater treatment using hybrid treatment schemes based on cavitation and Fenton chemistry: a review, Ultrason. Sonochem. 21 (2014) 1–14, https://doi.org/10.1016/j.ultsonch.2013.07.009.

[67] J. Basiri Parsa, S.A. Ebrahimzadeh Zonouzian, Optimization of a heterogeneous catalytic hydrodynamic cavitation reactor performance in decolorization of Rhodamine B: application of scrap iron sheets, Ultrason. Sonochem. 20 (2013) 1442–1449, https://doi.org/10.1016/j.ultsonch.2013.04.013.

[68] K.P. Mishra, P.R. Gogate, Intensification of degradation of Rhodamine B using hydrodynamic cavitation in the presence of additives, Sep. Purif. Technol. 75 (2010) 385–391, https://doi.org/10.1016/j.seppur.2010.09.008.

[69] S. Rajoriya, S. Bargole, V.K. Saharan, Degradation of a cationic dye (Rhodamine 6G) using hydrodynamic cavitation coupled with other oxidative agents: reaction mechanism and pathway, Ultrason. Sonochem. 34 (2017) 183–194, https://doi.org/10.1016/j.ultsonch.2016.05.028.

[70] Y.F. Ye, Y. Zhu, N. Lu, X. Wang, Z. Su, Treatment of rhodamine B with cavitation technology: comparison of hydrodynamic cavitation with ultrasonic cavitation, RSC Adv. 11 (2021) 5096–5106, https://doi.org/10.1039/d0ra07727e.

[71] L. Tan, S. Ning, X. Zhang, S. Shi, Aerobic Decolorization and Degradation of Azo Dyes by Growing Cells of a Newly Isolated Yeast Candida tropicalis TL-F1, Bioresour. Technol. (2013), https://doi.org/10.1016/j.biortech.2013.03.183.

[72] M. Sivakumar, A.B. Pandit, Wastewater treatment: a novel energy efficient hydrodynamic cavitational technique, Ultrason. Sonochem. 9 (2002) 123–131. http://www.ncbi.nlm.nih.gov/pubmed/12154685.

[73] D. Xu, H. Ma, Degradation of rhodamine B in water by ultrasound-assisted TiO_2 photocatalysis, J. Clean. Prod. 313 (2021), 127758, https://doi.org/10.1016/j.jclepro.2021.127758.

[74] M.a. Behnajady, N. Modirshahla, N. Daneshvar, M. Rabbani, Photocatalytic degradation of an azo dye in a tubular continuous-flow photoreactor with immobilized TiO_2 on glass plates, Chem. Eng. J. 127 (2007) 167–176, https://doi.org/10.1016/j.cej.2006.09.013.

[75] K.O. Badmus, N. Irakoze, O.R. Adeniyi, L. Petrik, Synergistic advance Fenton oxidation and hydrodynamic cavitation treatment of persistent organic dyes in textile wastewater, J. Environ. Chem. Eng. 8 (2020), 103521, https://doi.org/10.1016/j.jece.2019.103521.

[76] G.L. Maddikeri, A.B. Pandit, P.R. Gogate, Ultrasound assisted interesterification of waste cooking oil and methyl acetate for biodiesel and triacetin production, Fuel Process. Technol. 116 (2013) 241–249, https://doi.org/10.1016/j.fuproc.2013.07.004.

[77] A.L. Prajapat, P.R. Gogate, Intensification of depolymerization of aqueous guar gum using hydrodynamic cavitation, Chem. Eng. Process: Process Intensif. 93 (2015) 1–9, https://doi.org/10.1016/j.cep.2015.04.002.

[78] V.L. Gole, K.R. Naveen, P.R. Gogate, Hydrodynamic cavitation as an efficient approach for intensification of synthesis of methyl esters from sustainable feedstock, Chem. Eng. Process: Process Intensif. 71 (2013) 70–76, https://doi.org/10.1016/j.cep.2012.10.006.

[79] A.A. Pradhan, P.R. Gogate, Removal of p-nitrophenol using hydrodynamic cavitation and Fenton chemistry at pilot scale operation, Chem. Eng. J. 156 (2010) 77–82, https://doi.org/10.1016/j.cej.2009.09.042.

[80] C. Yi, Q. Lu, Y. Wang, Y. Wang, B. Yang, Degradation of organic wastewater by hydrodynamic cavitation combined with acoustic cavitation, Ultrason. Sonochem. 43 (2018) 156–165, https://doi.org/10.1016/j.ultsonch.2018.01.013.

[81] E. Cako, K. Fedorov, R. Darvishi, C. Soltani, A. Przyjazny, G. Boczkaj, Hydrodynamic cavitation based advanced oxidation processes : studies on specific effects of inorganic acids on the degradation effectiveness of organic pollutants, J. Mol. Liq. (2020) 307, https://doi.org/10.1016/j.molliq.2020.113002.

[82] P.R. Gogate, Cavitational reactors for process intensification of chemical processing applications: a critical review, Chem. Eng. Process: Process Intensif. 47 (2008) 515–527, https://doi.org/10.1016/j.cep.2007.09.014.

[83] S. Rajoriya, S. Bargole, V.K. Saharan, Degradation of reactive blue 13 using hydrodynamic cavitation: effect of geometrical parameters and different oxidizing additives, Ultrason. Sonochem. 37 (2017) 192–202, https://doi.org/10.1016/j.ultsonch.2017.01.005.

[84] L.V. Malade, U.B. Deshannavar, Decolorisation of reactive red 120 by hydrodynamic cavitation, Mater. Today Proc. 5 (2018) 18400–18409, https://doi.org/10.1016/j.matpr.2018.06.180.

[85] J. Zhang, J. Luo, Y. Wang, B. Dong, Z. Xu, L. Wang, A. Liu, Experimental investigation on characteristics of venturi cavitating flow and Rhodamine B degradation in methanol solution, Flow Meas. Instrum. 85 (2022), 102171, https://doi.org/10.1016/j.flowmeasinst.2022.102171.

[86] A.G. Chakinala, D.H. Bremner, P.R. Gogate, K.C. Namkung, A.E. Burgess, Multivariate analysis of phenol mineralisation by combined hydrodynamic cavitation and heterogeneous advanced Fenton processing, Appl. Catal., B 78 (2008) 11–18, https://doi.org/10.1016/j.apcatb.2007.08.012.

[87] A. V Mohod, P.R. Gogate, Ultrasonics -sonochemistry intensified synthesis of medium chain triglycerides using ultrasonic reactors at a capacity of 4L, Ultrason. Sonochem. 42 (2018) 347–355.

[88] E. Cako, K. Dinesh, R. Darvishi, C. Soltani, G. Boczkaj, Ultrafast degradation of brilliant cresyl blue under hydrodynamic cavitation based advanced oxidation processes (AOPs), Water Resour. Ind. 24 (2020), 100134, https://doi.org/10.1016/j.wri.2020.100134.

[89] B. Avvaru, A.B. Pandit, Experimental investigation of cavitational bubble dynamics under multi-frequency system, Ultrason. Sonochem. 15 (2008) 578–589, https://doi.org/10.1016/j.ultsonch.2007.06.012.

[90] P.R. Gogate, A.L. Prajapat, Depolymerization using sonochemical reactors: a critical review, Ultrason. Sonochem. 27 (2015) 480–494, https://doi.org/10.1016/j.ultsonch.2015.06.019.

[91] V.K. Saharan, A.B. Pandit, P.S. Satish Kumar, S. Anandan, Hydrodynamic cavitation as an advanced oxidation technique for the degradation of acid red 88 dye, Ind. Eng. Chem. Res. 51 (2012) 1981–1989, https://doi.org/10.1021/ie200249k.

[92] K. Fedorov, X. Sun, G. Boczkaj, Combination of hydrodynamic cavitation and SR-AOPs for simultaneous degradation of BTEX in water, Chem. Eng. J. 417 (2021), 128081, https://doi.org/10.1016/j.cej.2020.128081.

[93] M. Gągol, R.D.C. Soltani, A. Przyjazny, G. Boczkaj, Effective degradation of sulfide ions and organic sulfides in cavitation-based advanced oxidation processes (AOPs), Ultrason. Sonochem. 58 (2019), https://doi.org/10.1016/j.ultsonch.2019.05.027.

[94] P.B. Dhanke, S.M. Wagh, Intensification of the degradation of Acid RED-18 using hydrodynamic cavitation, Emerg Contam 6 (2020) 20–32, https://doi.org/10.1016/j.emcon.2019.12.001.

[95] D. Panda, S. Manickam, Hydrodynamic cavitation assisted degradation of persistent endocrine-disrupting organochlorine pesticide Dicofol: optimization of operating parameters and investigations on the mechanism of intensification, Ultrason. Sonochem. 51 (2019) 526–532, https://doi.org/10.1016/j.ultsonch.2018.04.003.

[96] P.R. Gogate, M. Sivakumar, A.B. Pandit, Destruction of Rhodamine B using novel sonochemical reactor with capacity of 7.5 l, Sep. Purif. Technol. 34 (2004) 13–24, https://doi.org/10.1016/S1383-5866(03)00170-9.

[97] D. Kobayashi, H. Matsumoto, Kinetics analysis for development of a rate constant estimation model for ultrasonic degradation reaction in the presence of particles, Chem Eng Trans 74 (2019) 571–576, https://doi.org/10.3303/CET1974096.

[98] O. Aguilar, C. Ángeles, C.O. Castillo, C. Martínez, R. Rodríguez, R.S. Ruiz, M.G. Vizcarra, On the ultrasonic degradation of Rhodamine B in water: kinetics and operational conditions effect, Environ. Technol. 35 (2014) 1183–1189, https://doi.org/10.1080/09593330.2013.864711.

[99] M. Sivakumar, a B. Pandit, Ultrasound enhanced degradation of Rhodamine B: optimization with power density, Ultrason. Sonochem. 8 (2001) 233–240. http://www.ncbi.nlm.nih.gov/pubmed/11441604.

[100] X. Zhang, C. Hao, C. Ma, Z. Shen, J. Guo, R. Sun, Studied on sonocatalytic degradation of Rhodamine B in aqueous solution, Ultrason. Sonochem. 58 (2019), 104691, https://doi.org/10.1016/j.ultsonch.2019.104691.

[101] M. Aliabadi, T. Sagharigar, Photocatalytic removal of rhodamine B from aqueous solutions using TiO_2 nanocatalyst, J. Appl. Environ. Biol. Sci. 1 (2011) 620–626. www.textroad.com.

[102] B. Bethi, G.B. Radhika, L.M. Thang, S.H. Sonawane, G. Boczkaj, Photocatalytic decolourization of Rhodamine-B dye by visible light active ZIF-8/$BiFeO_3$ composite, Environ. Sci. Pollut. Res. (2022), https://doi.org/10.1007/s11356-022-20165-6.

[103] N.S. Bhaskar, A.D. Kadam, J.J. Biwal, P.M. Diwate, R.R. Dalbhanjan, D.D. Mahale, S.P. Hinge, B.S. Banerjee, A. V Mohod, P.R. Gogate, Removal of Rhodamine 6G from wastewater using solar irradiations in the presence of different additives, Desalination Water Treat. (2015) 1–11, https://doi.org/10.1080/19443994.2015.1090923, 1090923.

[104] B.S. Banerjee, A.V. Khode, A.P. Patil, A.V. Mohod, P.R. Gogate, Sonochemical decolorization of wastewaters containing Rhodamine 6G using ultrasonic bath at an operating capacity of 2 L, Desalination Water Treat. 52 (2014), https://doi.org/10.1080/19443994.2013.786656.

[105] F.H. AlHamedi, M.A. Rauf, S.S. Ashraf, Degradation studies of Rhodamine B in the presence of UV/H_2O_2, Desalination 239 (2009) 159–166, https://doi.org/10.1016/j.desal.2008.03.016.

[106] S.K. Kansal, M. Singh, D. Sud, Studies on Photodegradation of Two Commercial Dyes in Aqueous Phase Using Different Photocatalysts, 19, 2006, https://doi.org/10.1016/j.jhazmat.2006.07.035.

[107] S.P. Hinge, M.S. Orpe, K.V. Sathe, G.D. Tikhe, N.S. Pandey, K.N. Bawankar, M.V. Bagal, A.V. Mohod, P.R. Gogate, Combined removal of Rhodamine B and Rhodamine 6G from wastewater using novel treatment approaches based on ultrasonic and ultraviolet irradiations, Desalination Water Treat. 57 (2016), https://doi.org/10.1080/19443994.2016.1143404.

[108] S. Zhang, L. Shen, W. Gong, Enhancing the Degradation of Rhodamine B by Hydrodynamic Cavitation with CCl4 Augmentation, Adv. Mater. Res. 867 (2014) 1244–1252. https://doi.org/10.4028/www.scientific.net/AMR.864-867.1244.

[109] K.P. Mishra, P.R. Gogate, Intensification of degradation of Rhodamine B using hydrodynamic cavitation in the presence of additives, Sep. Purif. Technol. 75 (2010) 385–391, https://doi.org/10.1016/j.seppur.2010.09.008.

[110] X. Chen, J. Dai, G. Shi, L. Li, G. Wang, H. Yang, Sonocatalytic degradation of Rhodamine B catalyzed by β-Bi_2O_3 particles under ultrasonic irradiation, Ultrason. Sonochem. 29 (2016) 172–177, https://doi.org/10.1016/j.ultsonch.2015.08.010.

[111] I.A. Pawar, P.J. Joshi, A.D. Kadam, N.B. Pande, P.H. Kamble, S.P. Hinge, B.S. Banerjee, A. V Mohod, P.R. Gogate, Ultrasonics Sonochemistry Ultrasound-based treatment approaches for intrinsic viscosity reduction of polyvinyl pyrrolidone (PVP), Ultrason. Sonochem. (2014), https://doi.org/10.1016/j.ultsonch.2013.12.013.

[112] A.V. Mohod, P.R. Gogate, Ultrasonic degradation of polymers: effect of operating parameters and intensification using additives for carboxymethyl cellulose (CMC) and polyvinyl alcohol (PVA), Ultrason. Sonochem. 18 (2011), https://doi.org/10.1016/j.ultsonch.2010.11.002.

[113] M. V Bagal, P.R. Gogate, Degradation of 2,4-dinitrophenol using a combination of hydrodynamic cavitation, chemical and advanced oxidation processes, Ultrason. Sonochem. 20 (2013) 1226–1235, https://doi.org/10.1016/j.ultsonch.2013.02.004.

[114] N. Barka, S. Qourzal, A. Assabbane, A. Nounah, Y. Ait-Ichou, Factors influencing the photocatalytic degradation of Rhodamine B by TiO_2-coated non-woven paper, J. Photochem. Photobiol. Chem. 195 (2008) 346–351, https://doi.org/10.1016/j.jphotochem.2007.10.022.

[115] N. Daneshvar, M. Rabbani, N. Modirshahla, M.A. Behnajady, Kinetic modeling of photocatalytic degradation of Acid Red 27 in UV/TiO_2 process, J. Photochem. Photobiol. Chem. 168 (2004) 39–45, https://doi.org/10.1016/j.jphotochem.2004.05.011.

[116] A.a. Pradhan, P.R. Gogate, Removal of p-nitrophenol using hydrodynamic cavitation and Fenton chemistry at pilot scale operation, Chem. Eng. J. 156 (2010) 77–82, https://doi.org/10.1016/j.cej.2009.09.042.
[117] P.N. Patil, P.R. Gogate, Degradation of methyl parathion using hydrodynamic cavitation: effect of operating parameters and intensification using additives, Sep. Purif. Technol. 95 (2012) 172–179, https://doi.org/10.1016/j.seppur.2012.04.019.
[118] R.K. Joshi, P.R. Gogate, Degradation of dichlorvos using hydrodynamic cavitation based treatment strategies, Ultrason. Sonochem. 19 (2012) 532–539, https://doi.org/10.1016/j.ultsonch.2011.11.005.
[119] K. Roy, V.S. Moholkar, p–nitrophenol degradation by hybrid advanced oxidation process of heterogeneous Fenton assisted hydrodynamic cavitation: discernment of synergistic interactions and chemical mechanism, Chemosphere 283 (2021), 131114, https://doi.org/10.1016/j.chemosphere.2021.131114.
[120] S. Raut-Jadhav, D. Saini, S. Sonawane, A. Pandit, Effect of process intensifying parameters on the hydrodynamic cavitation based degradation of commercial pesticide (methomyl) in the aqueous solution, Ultrason. Sonochem. 28 (2015) 283–293, https://doi.org/10.1016/j.ultsonch.2015.08.004.
[121] B.S. Banerjee, A. v Khode, A.P. Patil, A. v Mohod, P.R. Gogate, Sonochemical Decolorization of Wastewaters Containing Rhodamine 6G Using Ultrasonic Bath at an Operating Capacity of 2 L, 2013, 786656, https://doi.org/10.1080/19443994.2013.786656, 1–10.
[122] L.R. Bonetto, F. Ferrarini, C. De Marco, J.S. Crespo, R. Guégan, M. Giovanela, Removal of methyl violet 2B dye from aqueous solution using a magnetic composite as an adsorbent, J. Water Proc. Eng. 6 (2015) 11–20, https://doi.org/10.1016/j.jwpe.2015.02.006.
[123] S.P. Patil, V.S. Shrivastava, G.H. Sonawane, Photocatalytic degradation of Rhodamine 6G using ZnO-montmorillonite nanocomposite: a kinetic approach, Desalination Water Treat. 54 (2015) 374–381, https://doi.org/10.1080/19443994.2014.883334.
[124] F. Madjene, M. Assassi, I. Chokri, T. Enteghar, H. Lebik, Optimization of photocatalytic degradation of rhodamine B using Box–Behnken experimental design: mineralization and mechanism, Water Environ. Res. 93 (2021) 112–122, https://doi.org/10.1002/wer.1360.
[125] P.S. Bapat, A.B. Pandit, Thermodynamic and kinetic considerations of nucleation and stabilization of acoustic cavitation bubbles in water, Ultrason. Sonochem. 15 (2008) 65–77, https://doi.org/10.1016/j.ultsonch.2007.01.005.
[126] S.K. Kansal, M. Singh, D. Sud, Studies on photodegradation of two commercial dyes in aqueous phase using different photocatalysts, J. Hazard Mater. 141 (2007) 581–590, https://doi.org/10.1016/j.jhazmat.2006.07.035.
[127] Y. Gopalakrishnan, A. Al-Gheethi, R. Mohamed, N.H. Arifin, N.A. Salleh, Green ZnO nanoparticles photocatalyst for efficient BR51 degradation: kinetics and mechanism study, Environ. Prog. Sustain. Energy 40 (2021), https://doi.org/10.1002/ep.13559.
[128] N.B. Bokhale, S.D. Bomble, R.R. Dalbhanjan, D.D. Mahale, S.P. Hinge, B.S. Banerjee, A. V Mohod, P.R. Gogate, Ultrasonics Sonochemistry Sonocatalytic and sonophotocatalytic degradation of rhodamine 6G containing wastewaters, Ultrason. Sonochem. 21 (2014) 1797–1804, https://doi.org/10.1016/j.ultsonch.2014.03.022.
[129] D. Lutic, C. Coromelci-Pastravanu, I. Cretescu, I. Poulios, C.D. Stan, Photocatalytic treatment of rhodamine 6G in wastewater using photoactive ZnO, Int. J. Photoenergy (2012) 2012, https://doi.org/10.1155/2012/475131.
[130] U. Sirisha, B. Sowjanya, H. Rehana Anjum, T. Punugoti, A. Mohamed, M. Vangalapati, Synthesized TiO_2 nanoparticles for the application of photocatalytic degradation of synthetic toxic dye acridine orange, Mater. Today Proc. (2022), https://doi.org/10.1016/j.matpr.2022.04.278.
[131] V.L. Gole, P.R. Gogate, Sonochemical degradation of chlorobenzene in the presence of additives, Water Sci. Technol. 69 (2014) 882–888, https://doi.org/10.2166/wst.2013.790.
[132] J.A. Khan, M. Sayed, N.S. Shah, S. Khan, Y. Zhang, G. Boczkaj, H.M. Khan, D.D. Dionysiou, Synthesis of eosin modified TiO_2 film with co-exposed {001} and {101} facets for photocatalytic degradation of para-aminobenzoic acid and solar H2 production, Appl. Catal. B 265 (2020), https://doi.org/10.1016/j.apcatb.2019.118557.
[133] A. Fernandes, P. Makoś, Z. Wang, G. Boczkaj, Synergistic effect of TiO_2 photocatalytic advanced oxidation processes in the treatment of refinery effluents, Chem. Eng. J. 391 (2020), https://doi.org/10.1016/j.cej.2019.123488.
[134] A. Fernandes, M. Gągol, P. Makoś, J.A. Khan, G. Boczkaj, Integrated photocatalytic advanced oxidation system (TiO_2/UV/O_3/H_2O_2)for degradation of volatile organic compounds, Sep. Purif. Technol. 224 (2019) 1–14, https://doi.org/10.1016/j.seppur.2019.05.012.
[135] H. Zhao, G. Zhang, Q. Zhang, MnO_2/CeO_2 for catalytic ultrasonic degradation of methyl orange, Ultrason. Sonochem. 21 (2014) 991–996, https://doi.org/10.1016/j.ultsonch.2013.12.002.
[136] J. Ge, J. Qu, Degradation of azo dye acid red B on manganese dioxide in the absence and presence of ultrasonic irradiation, J. Hazard Mater. 100 (2003) 197–207, https://doi.org/10.1016/S0304-3894(03)00105-5.
[137] B. Çinar, I. Kerimoğlu, B. Tönbül, A. Demirbüken, S. Dursun, I. Cihan Kaya, V. Kalem, H. Akyildiz, Hydrothermal/electrospinning synthesis of CuO plate-like particles/TiO_2 fibers heterostructures for high-efficiency photocatalytic degradation of organic dyes and phenolic pollutants, Mater. Sci. Semicond. Process. 109 (2020), https://doi.org/10.1016/j.mssp.2020.104919.
[138] K. Li, Y. Wang, S. Wang, B. Zhu, S. Zhang, W. Huang, S. Wu, catalysts for low-temperature CO oxidation 18 (2009) 449–452, https://doi.org/10.1016/S1003-9953(08)60144-9.
[139] S.M. Grimes, H. Lateef, A.J. Jafari, L. Mehta, Studies of the effects of copper, copper(II) oxide and copper(II) chloride on the thermal degradation of poly(vinyl chloride), Polym. Degrad. Stabil. 91 (2006) 3274–3280, https://doi.org/10.1016/j.polymdegradstab.2006.06.010.
[140] Y. Çalışkan, H.C. Yatmaz, N. Bektaş, Photocatalytic oxidation of high concentrated dye solutions enhanced by hydrodynamic cavitation in a pilot reactor, Process Saf. Environ. Protect. 111 (2017) 428–438, https://doi.org/10.1016/j.psep.2017.08.003.
[141] S. Kaur, V. Singh, Visible light induced sonophotocatalytic degradation of Reactive Red dye 198 using dye sensitized TiO_2, Ultrason. Sonochem. 14 (2007) 531–537, https://doi.org/10.1016/j.ultsonch.2006.09.015.
[142] R.D.C. Soltani, Z. Miraftabi, M. Mahmoudi, S. Jorfi, G. Boczkaj, A. Khataee, Stone cutting industry waste-supported zinc oxide nanostructures for ultrasonic assisted decomposition of an anti-inflammatory non-steroidal pharmaceutical compound, Ultrason. Sonochem. 58 (2019), https://doi.org/10.1016/j.ultsonch.2019.104669.
[143] R.D.C. Soltani, M. Mashayekhi, M. Naderi, G. Boczkaj, S. Jorfi, M. Safari, Sonocatalytic degradation of tetracycline antibiotic using zinc oxide nanostructures loaded on nano-cellulose from waste straw as nanosonocatalyst, Ultrason. Sonochem. 55 (2019) 117–124, https://doi.org/10.1016/j.ultsonch.2019.03.009.
[144] V.K. Landge, S.H. Sonawane, M. Sivakumar, S.S. Sonawane, G. Uday Bhaskar Babu, G. Boczkaj, S-scheme heterojunction Bi_2O_3-ZnO/Bentonite clay composite with enhanced photocatalytic performance, Sustain. Energy Technol. Assessments 45 (2021), https://doi.org/10.1016/j.seta.2021.101194.
[145] R. Soltani, E. Abolhasani, M. Mashayekhi, G. Boczkaj, A. Khataee, Degradation of tetracycline antibiotic utilizing light driven-activated oxone in the presence of g-C_3N_4/ZnFe LDH binary heterojunction nanocomposite, Chemosphere 303 (2022), 135201, https://doi.org/10.1016/j.chemosphere.2022.135201.
[146] G. Li, L. Yi, J. Wang, Y. Song, Hydrodynamic cavitation degradation of Rhodamine B assisted by Fe3+-doped TiO_2: mechanisms, geometric and operation parameters, Ultrason. Sonochem. 60 (2020), 104806, https://doi.org/10.1016/j.ultsonch.2019.104806.
[147] M. Chen, K. Zhuang, J. Sui, C. Sun, Y. Song, N. Jin, Hydrodynamic cavitation-enhanced photocatalytic activity of P-doped TiO_2 for degradation of ciprofloxacin: synergetic effect and mechanism, Ultrason. Sonochem. 92 (2023), https://doi.org/10.1016/j.ultsonch.2022.106265.
[148] N.B. Bokhale, S.D. Bomble, R.R. Dalbhanjan, D.D. Mahale, S.P. Hinge, B.S. Banerjee, A.V. Mohod, P.R. Gogate, Sonocatalytic and sonophotocatalytic degradation of rhodamine 6G containing wastewaters, Ultrason. Sonochem. 21 (2014), https://doi.org/10.1016/j.ultsonch.2014.03.022.
[149] J. Wang, Z. Jiang, Z. Zhang, Y. Xie, X. Wang, Z. Xing, R. Xu, X. Zhang, Sonocatalytic degradation of acid red B and rhodamine B catalyzed by nano-sized ZnO powder under ultrasonic irradiation, Ultrason. Sonochem. 15 (2008) 768–774, https://doi.org/10.1016/j.ultsonch.2008.02.002.
[150] D. Xu, H. Ma, Degradation of rhodamine B in water by ultrasound-assisted TiO_2 photocatalysis, J. Clean. Prod. 313 (2021), 127758, https://doi.org/10.1016/j.jclepro.2021.127758.
[151] E. Pino, F. Herrera, G. Cifuentes, G. Arteaga, Photocatalytic degradation of aqueous rhodamine 6G using supported TiO_2 catalysts, A Model for the Removal of Organic Contaminants From Aqueous, Front. Chem. 8 (2020) 1–12, https://doi.org/10.3389/fchem.2020.00365.
[152] Z. Ait-Touchente, A.M. Khalil, S. Simsek, S. Boufi, L.F.V. Ferreira, M. Rei Vilar, R. Touzani, M.M. Chehimi, Ultrasonic effect on the photocatalytic degradation of Rhodamine 6G (Rh6G) dye by cotton fabrics loaded with TiO2, Cellulose 27 (2020) 1085–1097, https://doi.org/10.1007/s10570-019-02817-y.

[153] S. Salvi, P. Lokhande, H. Mujawar, Photodegradation of rhodamine 6G dye by Cd , Sr doped ZnO photocatalyst, Synthesized by Mechanochemical Method 137 (2017) 48–53.
[154] C. Lops, A. Ancona, K. di Cesare, B. Dumontel, N. Garino, G. Canavese, S. Hérnandez, V. Cauda, Sonophotocatalytic degradation mechanisms of Rhodamine B dye via radicals generation by micro- and nano-particles of ZnO, Appl. Catal., B 243 (2019) 629–640, https://doi.org/10.1016/j.apcatb.2018.10.078.
[155] S.C. M Akram, A. Chowdhuri, Environmental science : an Indian wastewater by ultrasound-assisted, Environ. Sci.: An Indian Journal. 12 (2016) 115–123.
[156] M.F. Hou, L. Liao, W. de Zhang, X.Y. Tang, H.F. Wan, G.C. Yin, Degradation of rhodamine B by Fe(0)-based Fenton process with H_2O_2, Chemosphere 83 (2011) 1279–1283, https://doi.org/10.1016/j.chemosphere.2011.03.005.
[157] X. Chen, Z. Xue, Y. Yao, W. Wang, F. Zhu, C. Hong, Oxidation degradation of rhodamine B in aqueous by UV/S $_2O_8^{2-}$ treatment system, Int. J. Photoenergy (2012) 2012, https://doi.org/10.1155/2012/754691.
[158] M.V. Bagal, P.R. Gogate, Wastewater treatment using hybrid treatment schemes based on cavitation and Fenton chemistry: a review, Ultrason. Sonochem. 21 (2014) 1–14, https://doi.org/10.1016/j.ultsonch.2013.07.009.
[159] X. Wang, J. Wang, P. Guo, W. Guo, C. Wang, Degradation of rhodamine B in aqueous solution by using swirling jet-induced cavitation combined with H_2O_2, J. Hazard Mater. 169 (2009) 486–491, https://doi.org/10.1016/j.jhazmat.2009.03.122.
[160] S. Wang, Q. Gong, J. Liang, Sonophotocatalytic degradation of methyl orange by carbon nanotube/TiO_2 in aqueous solutions, Ultrason. Sonochem. 16 (2009) 205–208, https://doi.org/10.1016/j.ultsonch.2008.08.002.
[161] P. Riesz, T. Kondo, FREE RADICAL FORMATION INDUCED BY ULTRASOUND AND ITS BIOLOGICAL IMPLICATIONS, 1992.
[162] M. Ashokkumar, J. Lee, S. Kentish, F. Grieser, Bubbles in an acoustic field: an overview, Ultrason. Sonochem. 14 (2007) 470–475, https://doi.org/10.1016/j.ultsonch.2006.09.016.
[163] B. Cuiping, X. Xianfeng, G. Wenqi, F. Dexin, X. Mo, G. Zhongxue, X. Nian, Removal of rhodamine B by ozone-based advanced oxidation process, Desalination 278 (2011) 84–90, https://doi.org/10.1016/j.desal.2011.05.009.
[164] A. Przyjazny, G. Boczkaj, Wastewater treatment by means of advanced oxidation processes based on cavitation, Review 338 (2018) 599–627, https://doi.org/10.1016/j.cej.2018.01.049.
[165] Z. Huang, F. Zhang, Y. Tang, Y. Wen, Z. Wu, Z. Fang, Rapid Degradation of Rhodamine B through Visible-Photocatalytic Advanced Oxidation Using Self-Degradable Natural Perylene Quinone Derivatives — Hypocrellins, 2022.
[166] P. Zawadzki, M. Deska, Degradation efficiency and kinetics analysis of an advanced oxidation process utilizing ozone, hydrogen peroxide and persulfate to degrade the dye rhodamine b, Catalysts 11 (2021), https://doi.org/10.3390/catal11080974.
[167] P. Zawadzki, Comparative studies of rhodamine b decolorization in the combined process $Na_2S_2O_8$/visible light/ultrasound, Desalination Water Treat. 213 (2021) 269–278, https://doi.org/10.5004/dwt.2021.26694.
[168] J. Gu, C. Luo, W. Zhou, Z. Tong, H. Zhang, P. Zhang, X. Ren, Degradation of Rhodamine B in aqueous solution by laser cavitation, Ultrason. Sonochem. 68 (2020), 105181, https://doi.org/10.1016/j.ultsonch.2020.105181.
[169] S.D. Ayare, P.R. Gogate, Sonochemical, photocatalytic and sonophotocatalytic oxidation of flonicamid pesticide solution using different catalysts, Chemical Engineering and Processing - Process Intensification 154 (2020), 108040, https://doi.org/10.1016/j.cep.2020.108040.
[170] S. Raut-Jadhav, V.K. Saharan, D.v. Pinjari, D.R. Saini, S.H. Sonawane, A.B. Pandit, Intensification of degradation of imidacloprid in aqueous solutions by combination of hydrodynamic cavitation with various advanced oxidation processes (AOPs), J. Environ. Chem. Eng. 1 (2013) 850–857, https://doi.org/10.1016/j.jece.2013.07.029.
[171] M.V. Bagal, P.R. Gogate, Degradation of diclofenac sodium using combined processes based on hydrodynamic cavitation and heterogeneous photocatalysis, Ultrason. Sonochem. 21 (2014) 1035–1043, https://doi.org/10.1016/j.ultsonch.2013.10.020.
[172] Z. He, S. Yang, Y. Ju, C. Sun, Microwave photocatalytic degradation of Rhodamine B using TiO_2 supported on activated carbon: mechanism implication, J. Environ. Sci. 21 (2009) 268–272, https://doi.org/10.1016/S1001-0742(08)62262-7.
[173] A.V. Mohod, A.C.S.C. Teixeira, M.V. Bagal, P.R. Gogate, R. Giudici, Degradation of organic pollutants from wastewater using hydrodynamic cavitation: A Review, J of environmental chemical engg. 11 (2023) 109773–109797, https://doi.org/10.1016/j.jece.2023.109773.
[174] T.S. Natarajan, M. Thomas, K. Natarajan, H.C. Bajaj, R.J. Tayade, Study on UV-LED/TiO2 process for degradation of Rhodamine B dye, Chem. Eng. J. 169 (2011) 126–134, https://doi.org/10.1016/j.cej.2011.02.066.
[175] P. Thanekar, M. Panda, P.R. Gogate, Degradation of carbamazepine using hydrodynamic cavitation combined with advanced oxidation processes, Ultrason. Sonochem. 40 (2018) 567–576, https://doi.org/10.1016/j.ultsonch.2017.08.001.
[176] S. Das, A.P. Bhat, P.R. Gogate, Degradation of dyes using hydrodynamic cavitation: process overview and cost estimation, J. Water Proc. Eng. 42 (2021), 102126, https://doi.org/10.1016/j.jwpe.2021.102126.
[177] G. Mancuso, M. Langone, M. Laezza, G. Andreottola, Decolourization of Rhodamine B: a swirling jet-induced cavitation combined with NaOCl, Ultrason. Sonochem. 32 (2016) 18–30, https://doi.org/10.1016/j.ultsonch.2016.01.040.
[178] R. Xu, R. Jiang, J. Wang, B. Liu, J. Gao, B. Wang, G. Han, X. Zhang, A novel method treating organic wastewater: air-bubble cavitation passing small glass balls, Chem. Eng. J. 164 (2010) 23–28, https://doi.org/10.1016/j.cej.2010.07.063.
[179] D.D. Mahale, N.N. Patil, D.S. Zodge, P.D. Gaikwad, B.S. Banerjee, K.N. Bawankar, A.V. Mohod, P.R. Gogate, Removal of patent blue V dye using air bubble-induced oxidation based on small glass balls: intensification studies, Desalination Water Treat. 57 (2016), https://doi.org/10.1080/19443994.2015.1075426.
[180] A.V. Mohod, S.P. Hinge, R.S. Raut, M.V. Bagal, D. Pinjari, Process intensified removal of methyl violet 2B using modified cavity-bubbles oxidation reactor, J. Environ. Chem. Eng. 6 (2018), https://doi.org/10.1016/j.jece.2017.12.053.
[181] M.P. Badve, P.R. Gogate, A.B. Pandit, L. Csoka, Hydrodynamic cavitation as a novel approach for delignification of wheat straw for paper manufacturing, Ultrason. Sonochem. 21 (2014) 162–168, https://doi.org/10.1016/j.ultsonch.2013.07.006.
[182] A.V. Mohod, P.R. Gogate, G. Viel, P. Firmino, R. Giudici, Intensification of biodiesel production using hydrodynamic cavitation based on high speed homogenizer, Chem. Eng. J. 316 (2017) 751–757, https://doi.org/10.1016/j.cej.2017.02.011.
[183] P.B. Patil, V.M. Bhandari, V. V Ranade, Chemical Engineering and Processing - process Intensification Wastewater treatment and process intensification for degradation of solvents using hydrodynamic cavitation, Chemical Engineering and Processing - Process Intensification 166 (2021), 108485, https://doi.org/10.1016/j.cep.2021.108485.
[184] M.T. Leal, M. Sa, E.R. Bandala, J. Matı, Solar Photocatalytic Degradation of Azo-Dyes by Photo-Fenton Process, 69, 2006, pp. 144–150, https://doi.org/10.1016/j.dyepig.2005.01.020.
[185] D.S. Bhatkhande, V.G. Pangarkar, A.A.C.M. Beenackers, Photocatalytic degradation of nitrobenzene using titanium dioxide and concentrated solar radiation, chemical effects and scaleup 37 (2003) 1223–1230.
[186] M. Hincapié, M.I. Maldonado, I. Oller, W. Gernjak, J.a. Sánchez-Pérez, M.M. Ballesteros, S. Malato, Solar photocatalytic degradation and detoxification of EU priority substances, Catal. Today 101 (2005) 203–210, https://doi.org/10.1016/j.cattod.2005.03.004.